ADVANCED HEALTHCARE MATERIALS
www.advhealthmat.de

Translating Therapeutic Microgels into Clinical Applications

Yonca Kittel, Alexander J. C. Kuehne, and Laura De Laporte**

Microgels are crosslinked, water-swollen networks with a 10 nm to 100 µm diameter and can be modified chemically or biologically to render them biocompatible for advanced clinical applications. Depending on their intended use, microgels require different mechanical and structural properties, which can be engineered on demand by altering the biochemical composition, crosslink density of the polymer network, and the fabrication method. Here, the fundamental aspects of microgel research and development, as well as their specific applications for theranostics and therapy in the clinic, are discussed. A detailed overview of microgel fabrication techniques with regards to their intended clinical application is presented, while focusing on how microgels can be employed as local drug delivery materials, scavengers, and contrast agents. Moreover, microgels can act as scaffolds for tissue engineering and regeneration application. Finally, an overview of microgels is given, which already made it into pre-clinical and clinical trials, while future challenges and chances are discussed. This review presents an instructive guideline for chemists, material scientists, and researchers in the biomedical field to introduce them to the fundamental physicochemical properties of microgels and guide them from fabrication methods via characterization techniques and functionalization of microgels toward specific applications in the clinic.

1. Introduction

Hydrogels are 3D hydrophilic macromolecular networks containing large amounts of water.[1–3] Bulk hydrogels are often employed for clinical applications; for example as lubricating coatings on catheters and medical devices, as therapeutic delivery depots, and as scaffolds for tissue engineering.[4,5] However, the macroscopic character of hydrogels limits the range of application to those listed above. Conversely, many modern therapeutic strategies require microscopic gel entities to take effect. Such microscopic gels—so called microgels—facilitate targeted systemic or on-site delivery, enables local imaging or allows for utilization of self-assembly and aggregation phenomena at a designated area in the body. Much like their macroscopic relatives, microgels are composed of water-soluble macromolecules that are crosslinked; however, they are much smaller than hydrogels with dimensions of the order of 10 nm to 100 µm. As such, microgels are sufficiently small to allow for injection, and depending on their size, circulation in the body. Microgels are adequately soft to conform to surfaces and cross membranes and biological barriers, and can be chemically modified to attach to biointerfaces, interact with biomolecules, or locally assemble into macroporous constructs.[6,7] Materials on the micro- or nanoscale exhibit fundamentally different properties and functions compared to macroscopic bulk materials, even when they are prepared from the same material. Therefore, microgels represent interesting materials for advanced clinical applications.[8,9] Depending on their application, microgels require different biochemical, mechanical, and structural properties, which can be engineered by altering the biochemical

Y. Kittel, A. J. C. Kuehne, L. De Laporte
DWI – Leibniz Institute for Interactive Materials
Forckenbeckstrasse 50, 52074 Aachen, Germany
E-mail: alexander.kuehne@uni-ulm.de; delaporte@dwi.rwth-aachen.de
A. J. C. Kuehne
Institute of Organic and Macromolecular Chemistry
Ulm University
Albert-Einstein-Allee 11, 89081 Ulm, Germany

The ORCID identification number(s) for the author(s) of this article can be found under https://doi.org/10.1002/adhm.202101989

DOI: 10.1002/adhm.202101989

A. J. C. Kuehne
Institute of Technical and Macromolecular Chemistry (ITMC)
Polymeric Biomaterials
RWTH University Aachen
Worringerweg 2, 52074 Aachen, Germany
L. De Laporte
Max Planck School-Matter to Life (MtL)
Jahnstraße 29, 69120 Heidelberg, Germany
L. De Laporte
Advanced Materials for Biomedicine (AMB)
Institute of Applied Medical Engineering (AME)
Center for Biohybrid Medical Systems (CBMS)
University Hospital RWTH
52074 Aachen, Germany

composition, crosslink density, and fabrication method. In addition, dynamic processes can be programmed into the microgels and triggered by internal stimuli (induced by the native environment) or by external stimuli (light, magnetic field, ultrasound, etc.).

Similar to hydrogels, microgels can be varied in their crosslink density, which alters the network porosity and morphology directly impacting on the softness, degree of swelling, stability, and potential degradation rate of the microgels.

Because of the importance of molecular structure and morphology to the properties of the microgel, the community combines these effects under the term internal structure.[10,11] The term internal structure unites the hierarchical contributions of molecular crosslink density and their morphological organization into a swollen microgel with different ratios of micro-, meso-, and macroporosity. While for solid state materials, there is a uniform IUPAC definition for micro- (<2 nm), meso- (2–50 nm), and macroporosity (>50 nm), there is no general definition for polymer networks.[12] In the literature one finds a suggestion for swollen soft materials, such as microgels, where the pore or mesh size for microporosity is defined as 10–100 nm and for macroporosity as 0.1–1 μm.[12] The porosity of the microgel polymer network can be adjusted. To avoid diffusion of specific molecules, such as outward diffusion of imaging units or inward diffusion of nucleases and proteases into microgels, a microporous polymer structure is needed,[13,14] while for cell infiltration and spreading, macroporosity in the polymer network is required, with pores even larger than 1 μm, obtained via network degradation or phase separation.[15,16] Alternatively, supramolecular interactions and dynamic covalent bonds can be employed that cells are able to break to remodel the hydrogel without the need for degradation or larger pores, yet these materials are mainly still bulk hydrogels.[17–19]

When microgel networks and their degradation products are nontoxic and exhibit a desirable biological response for a specific application, they are biocompatible. Their high water content and open-meshed structure offer many interesting functionalities, such as enabling diffusion of guest molecules, deformation to shapes deviating extremely from their relaxed state, and mimicking of the ECM.[2,20]

Depending on the type of molecular building blocks and their degree of crosslinking, microgels can have different properties and responsivity. The building blocks can be of natural origin, like sugars and proteins, or be synthetic, produced from artificial monomers, pre-polymers, and/or engineered peptides, proteins, and glycans. Many microgels consist of a hybrid composition of fused synthetic and natural functionalities to make use of the emergent synergistic effects.[21,22]

Here, we will first discuss the requirements for microgels to be applied in the body of a patient. Then we will give a detailed overview of the different existing technologies to produce microgels, followed by a discussion on how to characterize the microgels.

We provide an overview on how microgels can be employed as local drug or cell delivery vehicles, as scavengers to remove molecules from the body, or as probes that enable diagnostic visualization. Moreover, we discuss how microgels can act as scaffolds that provide structure to support tissue healing and regeneration.[23]

Finally, an overview will be given of those applications that have already made it into pre-clinical and clinical trials.

Along this train of thought, we will highlight existing challenges and chances for future applications.

Existing reviews about microgels focus on their mechanical and physicochemical properties.[24–26] There are also reviews about the potential applications of microgels[27–36] also in the biomedical field.[37–47] However, the community is lacking an instructive review that covers the requirements for microgels to be employed in the human body, while at the same time discussing which approaches have already translated into preclinical studies as well as clinical applications. The review at hand fills this gap, making it an important guideline for chemists, material scientists, and researchers in the biomedical field.

2. Requirements for Clinical Application

To enable clinical application like drug delivery systems, imaging probes, or building blocks for tissue regeneration scaffolds, microgels need to meet several criteria (see **Figure 1**).

2.1. Biocompatibility

Biocompatibility describes the ability of a material to perform with an appropriate host response in a specific application.[48] A more simplistic definition is that a material does not create any adverse tissue reactions, so any toxic effects to the body. In general, it is described in literature that noncharged microgels that are hydrophilic and swollen show high biocompatibility.[49] However, depending on the application of the microgels in vivo, the biocompatibility of the used polymer and thus the immune response of the body that is generated by the foreign material can change with the nature of the tissue, such as dermis, muscle, or adipose tissue.[50] For example, it is known that the brain does not form fibrotic scars. Poly(ethylene glycol) (PEG)-based materials are known to be biocompatible for in vivo applications; but they have also demonstrated to trigger fibrosis.[51] Therefore, polymer materials are functionalized with biocompatible molecules, such as proteins, to enhance biointegration.

2.2. Biodegradability

For most applications, the degradation products of the microgels need to be cleared from the body after the microgels have fulfilled their function. The degradation of a microgel network can occur via oxidative/reductive, hydrolytic, or enzymatic cleavage or via thermal- or photo-degradation, induced for example by laser irradiation.[52–56] The resulting degradation products should be smaller than 4 nm to be excreted renally (through the kidneys) and induce minimal cytotoxic effects and immune response, such as inflammation.[57] The way of molecular breakdown, as well as the degradation rate of the microgel network, are both highly dependent on the chemical and internal structure of the microgel. The crosslink density and swelling capacity of the microgel influence the thermodynamic bond stability as well as the degradation kinetics by affecting diffusion of the degradation

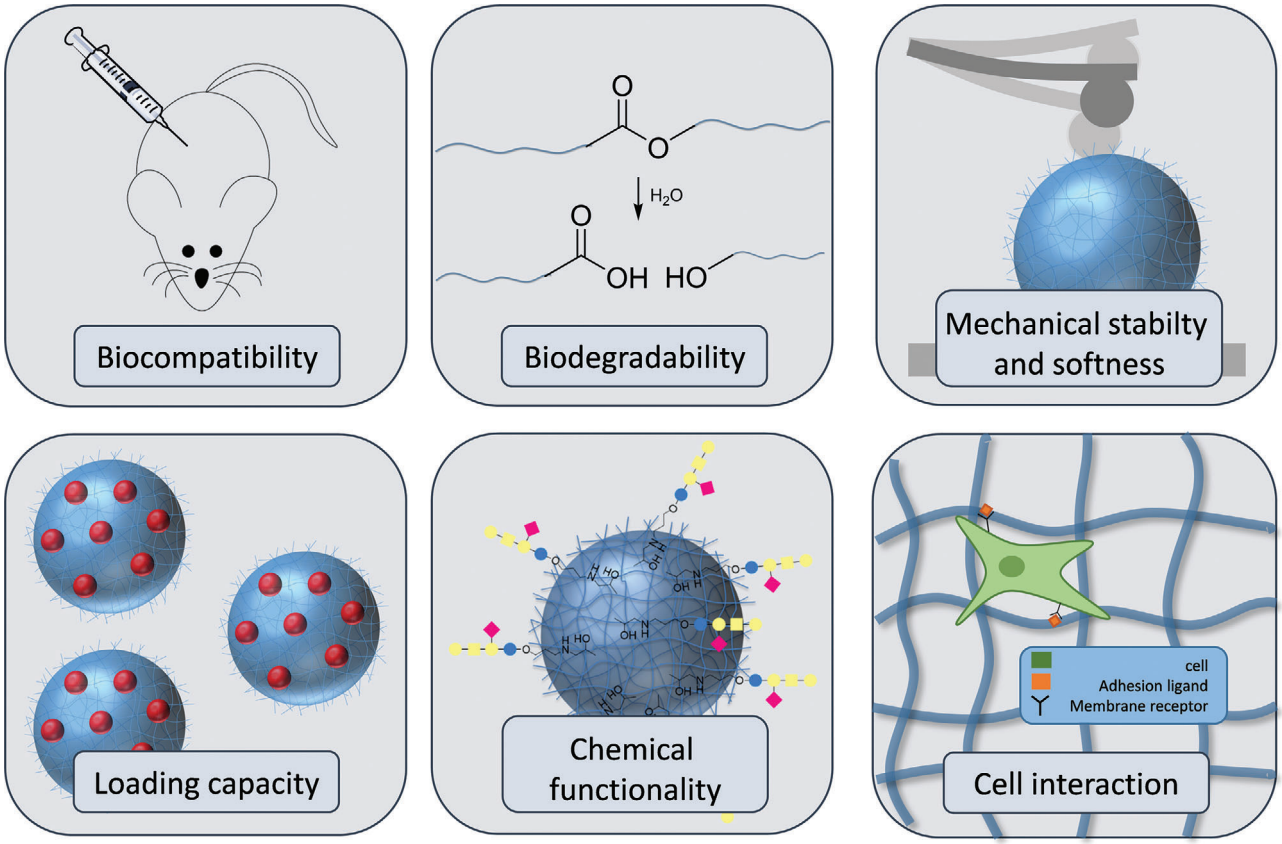

Figure 1. Overview of microgel requirements for clinical applications.

trigger (for example hydrolytic enzymes) or uptake of water, acid, or base required for hydrolysis.[52]

Therefore, microgel degradation can be programmed on a molecular level, by using appropriate hydrophilic monomers and polymers that are precisely suited for the desired biomedical application.[50] The degradation time of PEG-based microgels can range from minutes to years depending on the choice of degradable connectors or crosslinkers. Therefore, the speed of degradation can be adjusted to the desired short- or long-term biomedical application.[52,58,59] For rapid degradation, a Michael-type addition between acrylate and thiol can be used, while free radical polymerization of PEG diacrylate (PEGDA) is employed to enable slow degradation through ester hydrolysis at the sterically protected acrylate end-groups.[58,59] In vivo degradation experiments where PEGDA has been compared to PEG diacrylamide (PEGDAA) showed significant degradation of PEGDA samples after 12 weeks, while no measurable degradation could be detected for samples made of PEGDAA.[58] Instead of hydrolytically cleavable moieties, enzyme-sensitive domains can be incorporated between crosslinks to induce degradation upon exposure to the respective enzyme.[60] Importantly, the size of the degradation products is determined by the design of the chosen molecular architecture of the microgel. Star-shaped molecules with the same molecular weight as linear molecules will produce degradation products of smaller hydrodynamic radii, which are cleared faster from the body.[61,62]

2.3. Mechanical Stability and Softness

For many in vivo applications, microgels need to exhibit sufficient mechanical stability or softness to fulfil the respective task in the body.[50] The mechanical properties of the microgels, namely, softness or stiffness and in a related sense also their swelling behavior, can be adjusted by the backbone and crosslink density of the gel.[50] In addition, the type of crosslinking, being either covalent, dynamic covalent, or noncovalent, determines the viscoelastic behavior of the microgel.[63–66] For example, for the treatment of wound-triggered hemostasis, ultrasoft, highly deformable platelet-like microgels are investigated.[67] It is shown in dissipative particle dynamics simulations, that ultralow crosslinked polyNIPAM microgels (≈10 kPa) lead to an increase in clot concentration that reduces the bleeding time.[67,68] By contrast, in locations, such as the heart or the gastrointestinal tracts, higher shear forces are present leading to the requirement of stiffer microgels in the range of kPa up to MPa.[50,69,70]

2.4. Loading Capacity

One major advantage of microgels is their reversible swelling behavior, which makes them highly suitable for incorporation, storage, and delivery of cells, bio-macromolecules, therapeutic proteins, as well as drug molecules.[71] For delivery, microgels can be

swollen and loaded outside of the body. Collapse of the loaded microgel leads to encapsulation of the cargo. In the body, the microgel can be reswollen upon issuing a trigger release of the cargo. Triggers can be pH, redox, light, temperature and other chemical or physical leads.[72]

The encapsulation efficiency is determined by several factors:

- The internal structure influences the capacity of the microgel. Depending on the mesh size of the network the loaded molecules can diffuse more or less deep into the microgel. Finer meshes with higher nanoporosity can take up more molecular cargo than a microporous microgel, which in turn might be more suitable for encapsulation of cell cargo.[73–75]
- Functional groups presented throughout the microgel can increase the interaction with the respective cargo and hence increase the loading capacity. Due to the open network structure of the microgel, functionalization on "the inside" of the microgel allows for loading capacities surpassing those of solid and mesoporous particles.[27,45]
- Moreover, the heterogeneity of the microgel influences the loading capacity of the microgel. Heterogeneity can often occur as a gradient in structure or functionalization. Heterogeneity is evoked by changing reaction rates or phase separation of the building blocks upon polymerization. While a functionalization gradient limits the capacity toward the inside or (more often) toward the periphery of the microgel, a crosslinking gradient affects diffusion of cargo molecules deep into the microgel. On the other hand, a heterogeneous polymeric network leading to larger pores can enhance diffusion.[25]

2.5. Chemical Functionality

To direct microgels to their site of action, microgels can be functionalized with targeting units. To enable specific binding to biological interfaces the targeting units need to be attached only in the periphery of the microgel. Specific recognition motifs are often small peptides, glycans or DNA fragments, which bind to surface motifs presented by specific cells or at defined pathological sites in the body. This targeting enhances the selectivity of drug administration and thus the therapeutic efficacy.[71] Here, a remaining challenge is to keep the functional domains available for binding and avoid formation of a protein corona on the microgels when the get in touch with bodily fluids for example in the blood stream.[76] Moreover, microgels can be functionalized to interact with soluble molecules, for example with the glycosphingolipid receptor GM1a to effectively bind cholera toxin for the treatment of bacteria induced diarrhea.[77] It was shown that the microgels could scavenge cholera toxin in direct binding competition to colorectal cell, which demonstrate their great potential as a nonantibiotic treatment for toxin-mediated infectious disorders.

2.6. Cell Interaction

As an alternative to molecular drug delivery, therapeutic microgels can also be designed to interact with cells for regenerative purposes or immune modulation. Microgels can present antigenic proteins, nucleotides, drugs, and ECM components to interact with intracellular or surficial receptors on host cells.[78] Functional microgels can modulate the immune system in two ways:[50,79] First, immune cell activation can be down-regulated in hyperactive immune conditions, for example in autoimmune and inflammatory diseases. Second, immune cell activation is enhanced to reverse hypoactive immune responses for example in cancer or in chronic infections.[79] In the case of tissue engineering, aligned rod-shaped microgels inside of a gel matrix have been modified with Gly-Arg-Gly-Asp-Ser (GRGDS)-peptides, leading to enhanced fibroblast alignment due to strong interactions between the cells and the biofunctionalized microgels.[80]

Moreover, cells can be loaded inside microgels before injection into the body. Cellular therapy plays an important role in modern medicine for the treatment of cancer and cardiac diseases but remain very expensive, while most cells lose their effectiveness shortly after injection.[81,82] When unprotected cells are injected into the body, they are exposed to high shear and oxidation stresses, which deteriorate their fate and limit therapeutic efficiency. 80% of the cells undergo cell death or migrate away from the intended site of action.[83,84] Therefore, it is necessary to protect the cells by encapsulation into microgels.[85] The advantage of microgel encapsulation is the softness of the gel and its open degradable mesh structure, which supports all necessary functions of the cell and enables facile exchange of nutrients and metabolites. Microgels can bind to a targeted site and retain the cell locally.

Designing of cytocompatible microgels opens new possibilities for tissue engineering and applications in regenerative medicine.[86] They can function as building blocks and assemble into 3D regenerative constructs with or without cell encapsulation. The micron scaled interstices between the individual assembled microgels facilitate cell infiltration and growth.[87] The cytocompatibility of a microgel is given by its specific molecular interactions at the cell-microgel interface.[20] Successful microgel scaffolds are ECM-mimetics promoting cell adhesion, proliferation, migration, or differentiation of cells by attachment of the respective biomolecular cues to the microgels.[20,88] Arginine-glycine-aspartate (RGD) peptides are coupled to microgels to promote cell adhesion via integrin binding.[37,50] Recently, microgels have been implemented in bioinks to create 3D multifunctional scaffolds with properties that are typically found in native tissue.[89] Cell-laden microgels can be mixed with an injectable hydrogel precursors formulated as a bioink, enabling printing of *ex vivo* tissue models.[37,89] These multiscale 3D microgel-in-hydrogel biomaterials can be used to recreate the meso-environmental interplay of co-cultured cells, for example, with one microenvironment supporting tumor spheroid formation of cancer cells and one microenvironment supporting capillary network formation of vascular endothelial cells.[90]

3. Microgel Fabrication

In general, chemically crosslinked (macroscopic) hydrogels are prepared in two different ways: Either, via a step-growth polymerization or chain-growth polymerization. The same is true for the preparation of microgels, where often step-growth via Michael addition is employed or a free radical chain-growth polymeriza-

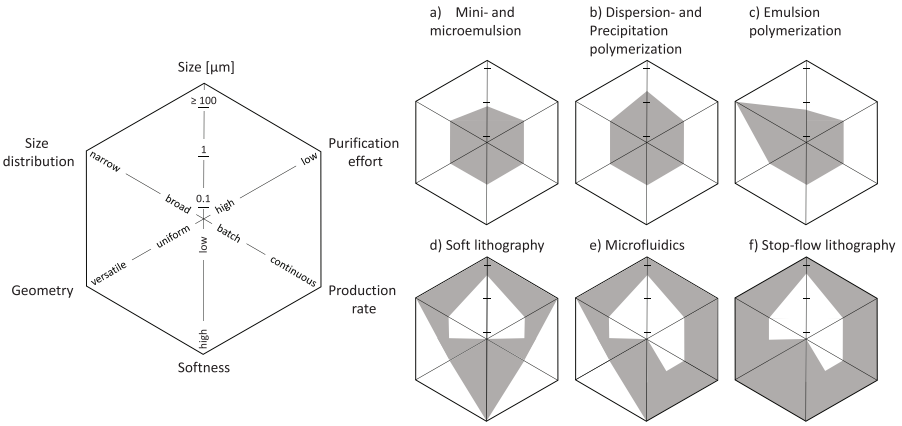

Figure 2. Key attributes of different microgel fabrication techniques.

tion is used. The two different growth mechanisms entail disparate internal structures and morphologies.[91] In step-growth polymerization, hydrophilic poly-functional molecules link together to form a well-controlled homogeneous or more heterogeneous network above or below the critical concentration, respectively; while in free-radical polymerization, reactive monomers link-up to form a molecular chain with statistically distributed crosslinking points, resulting in a gel of heterogeneous structure and crosslink density and often gradients.

Different fabrication techniques are available to prepare microgels depending on their size, shape, production rate, and mechanical stability and softness.[10] Submicrometer microgels are typically produced by free radical synthesis following dispersion-, precipitation-, and emulsion-polymerization, or polymerization in inverse mini- and microemulsion.[92] Larger microgels are produced via soft lithography, microfluidics, and SFL. In the following, we discuss the advantages and disadvantages of the different microgel fabrication techniques, while we give an overview of their respective key attributes in **Figure 2**.

3.1. Mini- and Microemulsion

For the production of microgels with diameters between 50 and 500 nm, polymerization in inverse miniemulsion can be employed.[92] Here, a water-in-oil (w/o) emulsion is formed with aqueous droplets containing water-soluble monomers dispersed in a nonpolar continuous phase.[93] The thermodynamic stability of an inverse miniemulsion is conveyed by the presence of a surfactant, which needs to be removed in a purification step after microgels have been obtained.[94]

Using an inverse microemulsion as a template for the polymerization of microgels allows for even smaller diameters between 10 and 100 nm; however, this requires surfactant levels above the critical micelle concentration (CMC).[94] Both methods deliver spherical microgels, as determined by the shape of the stabilized droplets.

3.2. Dispersion- and Precipitation Polymerization

Dispersion- and precipitation polymerization can be used for the production of microgels with diameters in the submicrometer to micrometer regime between 0.1 and 15 µm. process.[6,25,95] In both dispersion- and precipitation polymerization, the starting materials are dissolved in a solvent, in which initiation of the polymerization takes place. Collapsed microgel particles form upon phase inversion when the dissolved polymers reach a critical molecular weight. Dispersion polymerization is conducted in the presence of a stabilizing agent yielding monodisperse microgels, whereas in precipitation polymerization there is no additional agent leading to less uniform size distributions with microgel sizes between 0.1 and 8 µm.[96,97] Again, the shape of the resulting microgels is limited to spheres as this represents the lowest surface energy upon phase inversion from a homogeneous solution.

3.3. Emulsion Polymerization

Precisely monodisperse microgels can be produced using emulsion polymerization.[98] Emulsion polymerization is usually conducted by using hydrophobic monomers that are polymerized inside of micelles in the presence of a polar solvent. The monomers are prepared to switch from hydrophobic during polymerization to hydrophilic to obtain microgels by swelling in water post polymerization.[99] During synthesis, hydrophobic monomer diffuses steadily through the polar solvent and into the micelles to maintain growth of the particles by a radical polymerization.[99] To obtain microgels, the particles containing hydrophobic polymers are transferred into the hydrophilic state by deprotecting monomers or by charging them up by means of pH activation. Using this technique, extremely narrowly dispersed microgels in the range of hundreds of nanometers have been obtained.

Microgels with dimensions across the entire micrometer range can be fabricated by photolithography, in-mold polymerization, microfluidics, or stop flow lithography.

3.4. Photolithographic Techniques

Photolithographic techniques can be used to produce microgels with complex 2D geometries.[100] In photolithography, a light-sensitive photoresist (monomers or prepolymers; pure or in solution) is spin-coated onto a substrate (often a glass or silicon

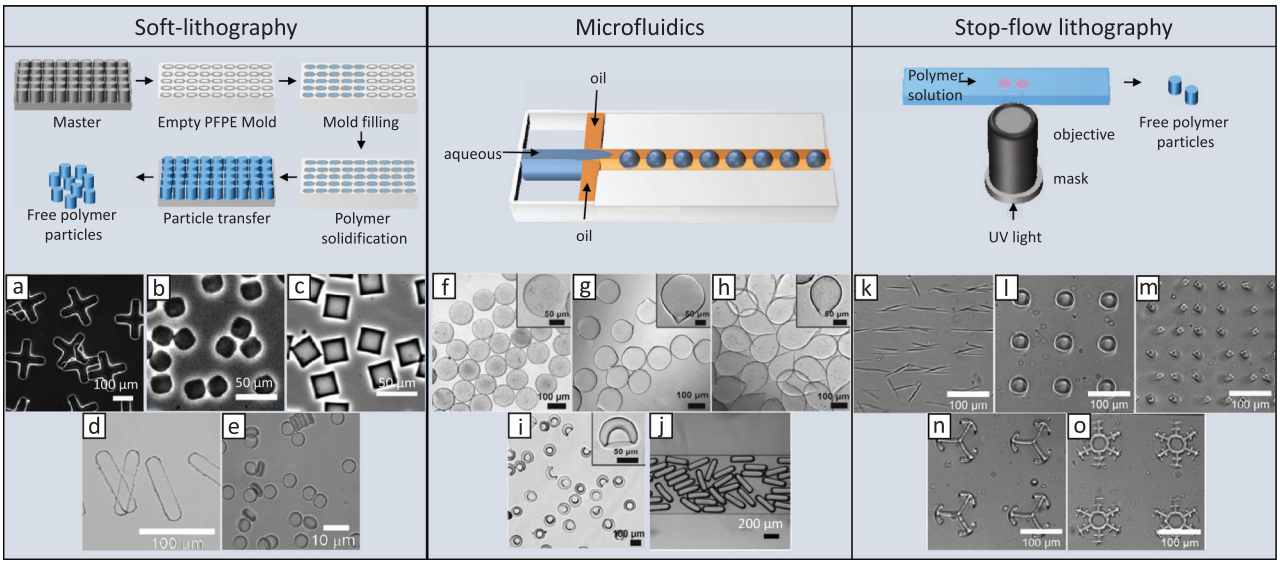

Figure 3. Microgel fabrication techniques: Left—Schematic of a soft-lithography process such as PRINT. a–e) Different microgel shapes accessible via PRINT: crosses, truncated cylinders, cubes, rods, and discs. Reproduced with permission.[298] Copyright 2006, Elsevier. Middle—Droplet-based microfluidic device. f–i) Cured microgels as spheres, droplet, and bowl shapes produced by on-chip polymerization. Reproduced with permission.[299] Copyright 2012, AIP Publishing. j) Microgel rods produced by on-chip curing under plug-flow conditions. Reproduced with permission.[84] Copyright 2019, Wiley-VCH GmbH. Right—Stop-flow lithography inside microfluidic channels. k–o) High aspect ratio microgel rods, spheres, cubes and cuboids, rotor and snowflake shapes. Reproduced with permission.[111] Copyright 2020, The Royal Society of Chemistry.

wafer). Patterns are generated by exposing the photoresist with UV light through an appropriate photomask. The exposed areas crosslink, the unexposed photoresist is removed by a "developer" solvent resulting in the desired patterns.[100]

Exposure to water leads to swelling of the produced crosslinked polymer networks and their detachment from the wafer. This method allows the production of monodisperse microgels with tailored sizes and geometries in the µm to mm range. However, some of the required manufacturing steps, such as UV-exposure, baking at high temperatures, and development with solvents, are incompatible with biological compounds and cells as they lead to biomolecular denaturation and cell death.[100] Therefore, folded biomolecules and cells have to be added post-fabrication and purification. Moreover, classical photolithography as borrowed from the microfabrication community gives only little control over the specific surface chemistry.[100]

3.5. Soft Lithography

Soft lithography provides an alternative to photolithography, which avails pattern-transfer by molding using elastomeric biocompatible materials.[100] PRINT (particle replication in nonwetting templates) is an advanced soft lithographic micromolding technique to produce monodisperse (sub)micrometer-sized microgels with control over particle size, geometry, composition, and functionality (see **Figure 3**a–e).[100] A mold produced from elastomeric perfluoropolyether (PFPE) or polydimethylsiloxane (PDMS) with defined cavities is filled with a polymer precursor solution. Crosslinking can take place via free-radical or step-growth polymerization and is initiated by temperature or light, leading to the formation of microgels that take the shape of the mold cavities.[92] This method additionally allows for the production of multi-compartment microgels with different functionalities in the core and on the surface through consecutively polymerizing different layers of subsequently adding polymer precursor solutions.[101] However, the evaporation of the solvent due to the small volumes of polymer precursor solution in mold polymerization can also lead to incompletely casted microgels for solutions with low polymer concentrations. To overcome this challenge, nonvolatile and nonreactive polymer fillers can be employed, which is washed out and replaced by water in by subsequent purification.[11,102] Altogether, photolithography, soft lithography, and PRINT are time consuming batch processes that are best suited for laboratory scale production rates.

3.6. Microfluidics

For continuous high-throughput production of monodisperse microgels larger than 10 µm, microfluidic techniques can be used.[92,103] Microfluidic devices are usually fabricated by soft lithography using PDMS, which is bonded to a glass substrate. Droplets are formed at the junction of two channels containing immiscible liquids, usually a continuous, surfactant containing oil phase and an aqueous polymer precursor solution. The polymer precursor droplets can be crosslinked to spherical microgels by chemical reactions, oftentimes initiated by UV light (e.g., photo-Diels-alder, radical polymerization, thiol-ene click) or ions (e.g., for alginate gels), or by 2 component mixing (for example Michael-type addition) (see Figure 3f–i).[84,92,104] Supramolecularly crosslinked microgels have been prepared on-chip via hydrogen bonding and hydrophobic interactions. These microgels degrade at increased pH. By varying the geometry of the microflu-

idic device, the flow rates and viscosities of the liquids, and the reaction times, microgels with different geometries and morphologies can be formed.[92,103] On-chip gelation allows crosslinking of the droplets inside of the channels during flow, where the microgels take the shape of the droplet, which may be confined and elongated in the channel. On-chip gelation can therefore yield anisometric microgel rods or disks (see Figure 3j).[84] Multifunctional anisometric Janus microgels with more complex structures can be generated by combining multiple aqueous and oil phases at different flow velocities. The use of multiple channels enables the formation of water-in-oil-in-water (w/o/w) double emulsion to generate hollow microgels, which can be used to encapsulate biomolecules on chip for drug delivery.[105,106] The possibility to use mild reaction conditions in microfluidics renders this technique ideal for incorporation of sensitive bioactive molecules, as well as cells into the microgels.[84,107–109] However, the microfluidic technique shows limitation as the geometry and size of the microgels are dictated by the dimensions and cross-section of the microfluidic channels.[10] To overcome this constraint, a technique to produce rod-shaped microgels with significantly smaller diameter than the channel diameter has been developed by operating a microfluidic chip in the jetting regime rather than the dripping regime. The jet containing the microgel precursors is exposed to a pulsed high intensity light source, ideally a laser.[10] The jet polymerizes only in the exposed segments leading to narrow rods of high aspect ratio and tunable lengths depending on the on-time of the laser and the jet velocity.

3.7. Stop-Flow Lithography

Stop-flow lithography (SFL) is a microfluidics-based method combined with photolithography for continuous high-throughput production of soft, anisometric, and multifunctional microgels with more complex geometries, morphologies, and chemical patterns (see Figure 3k–o).[110,111] A photo-crosslinkable precursor solution is guided through a microfluidic channel, while patterned UV light irradiates the solution through a mask, by using micro-LED- or micro-mirror displays or direct laser writing techniques. The flow is stopped while the channel segment is exposed to light to form microgels. The produced microgels are moved away from the exposure site by switching the flow on. Synchronizing flow-stopping and starting, light exposure, and channel flushing can lead to acceptable production rates of arbitrarily shaped 2D microgels.[110]

In the future, the advances in 3D stereolithography will be also transferred to hydrogel and microgel research enabling 3-dimensionally patterned microgels, higher production rates, while at the same time preventing clogging.[112] These microgels will provides new possibilities in biomedical engineering and responsive microgels.[111,113]

Importantly, the type of microgel fabrication technique also has an impact on the internal structure of the microgel. While dispersion-, precipitation- and emulsion polymerization yield microgels that often have a more densely crosslinked core and a loosely crosslinked periphery, which is fuzzy with many dangling chains (see **Figure 4**a–c), heterophase and confined approaches as in miniemulsions, jet-polymerization, PRINT, and droplet microfluidics lead to a more homogeneous distribution of crosslinks (see Figure 4d–k). Furthermore, the use of inert fillers, lithographic patterning, and shearing of the precursor solution during crosslinking or network formation have an impact on the internal structure (see Figure 4d–i).

4. Microgel Characterization

While microgel sizes range between 10 nm to 100 µm, the individual chain segments in the microgels are "dissolved," which is why microgels have properties connected to the molecular nature of the material, as well as the colloidal nature connected to their size and shape. Microgels can be envisioned as giant solubilized crosslinked macromolecules, which lack a defined surface. This means that any functional group that has been introduced might not only be exposed on the outside (as they would be in hard particles) but also on the inside of the microgel—significantly increasing the surface area for presenting these domains and therefore the binding capacity for the targeted molecules or binding motifs.

Depending on the network porosity and crosslink density, these functionalities are more or less well accessible for molecules or entities to bind to. These unique properties set microgels apart from hard colloidal and granular particles as well as macroscopic bulk hydrogels.[6,114–116]

The different structural properties of the microgels require suitable characterization methods for their analysis (**Table 1**)—naturally these are coming from the realms of molecular and colloidal materials but also from cellular characterization as there are many similarities between soft microgels and cells.[117–120]

4.1. Microgel Size, Size Distribution, and Microgel Aggregates

Microgel size, size distribution, and microgel aggregates can be easily and rapidly analyzed using dynamic light scattering (DLS) or static light scattering (SLS) methods.[121–123] This is most suitable for spherical microgels with diameters in a range of 1 nm to 5 µm. These techniques are noninvasive and nondestructive. Microgels are irradiated by a coherent light source, such as a laser, while the scattering angle as well as the intensity of the scattered light are measured.[138] DLS measures the time-dependent fluctuations in the scattering intensity, while SLS records the time-averaged intensity of scattered light. DLS is typically measured at a fixed angle, while SLS is measured over a set of different angles. DLS gives better information about the size (radius, diameter) of a narrowly dispersed set of microgels, SLS gives better information about the distribution of sizes.

During DLS measurement, the charge of microgels can be determined by measuring their electrophoretic mobility in the presence of an electric field.[123]

With these methods, also the size and change of stimuli-responsive microgels upon switching of the pH and temperature can be measured.[27] For the analysis of nonspherical microgels, multi-polarization DLS can be employed. Multi-polarization DLS is a modern approach, which is based on time-resolved measurements of the scattered light intensity at different angles between the incident and scattered light polarizations.[139] However, light scattering techniques should not be employed for microgels larger than 5 µm. For those microgels, optical microscopy can be used for size determination.[121]

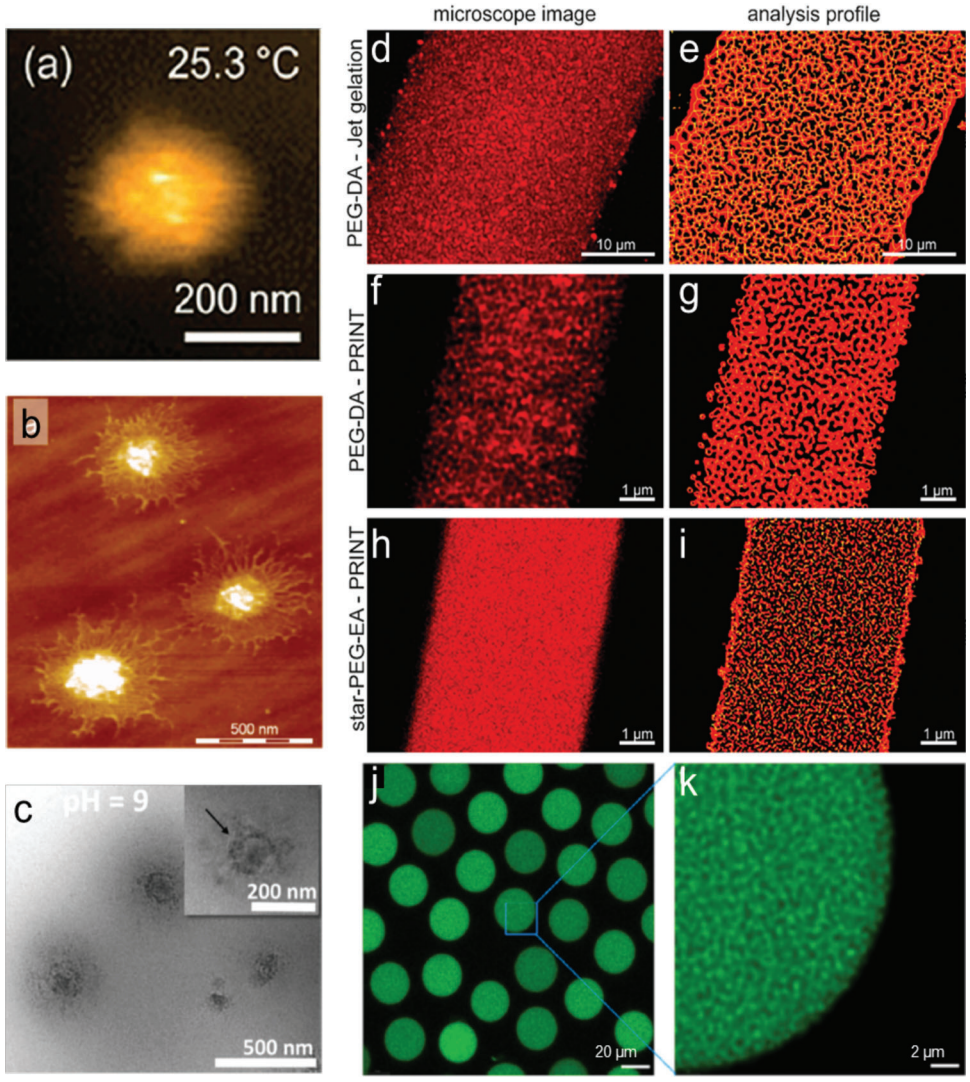

Figure 4. Internal structure influenced by different processing techniques and different analytical techniques. a) Precipitation synthesis of an NIPAM microgel in the swollen state analyzed by in situ AFM. The height profile displays a denser network in the center of the microgel. Reproduced with permission.[300] Copyright 2019, Wiley-VCH GmbH. b) Ultrasoft microgels analyzed by AFM clearly showing a denser core with a thin and surface-spreading shell. The fringes and indiscrete perimeter hint at a fuzzy periphery and Individual dangling chains. Reproduced with permission.[301] Copyright 2016, American Chemical Society. c) Microgels prepared by emulsion polymerization followed by deptrotection and swelling. The cryoTEM images display more contrast in the center and fading contrast toward the outside of the microgel, representing a material density gradient toward the outside also reflecting that there is more crosslinks toward the center of the microgel. Reproduced with permission.[98] Copyright 2015, The Royal Society of Chemistry. d) Microgel rod polymerized by exposure to a strong laser while in the jetting regime inside of a microfluidic device. The deconvolved confocal microscopy images of the fluorescently labeled microgel network display a homogeneous pore size distribution and the image analysis. e) The structure exhibits a skin on the outside, so will be less accessible from uptake. f,g) Deconvolved confocal micrograph on di-functional PEG chain that has been gelled in a PRINT mold. The image shows an open network structure with larger pores and voids as compared to the rod in (d/e). h/i) Same experiment as in (f/g) only with a star-shaped precursor molecules producing also a homogeneous pore-size distribution; however, with much smaller pores than in (f/g). (d/e/f/g/h/i): Reproduced with permission.[10] Copyright 2019, Wiley-VCH GmbH. j) Spherical microgels of a star-shaped PEG precursor produced by droplet microfluidics. k) Deconvolved confocal microscopy image of the internal microgel structure showing a homogeneous distribution of pores in the same range as the star-shaped PEG microgel produced by PRINT (h/i). (j/k): Reproduced with permission.[77] Copyright 2019, American Chemical Society.

4.2. Morphology, Homogeneity, and Chain Dynamics

Microgels are often used as drug delivery vehicles with incorporated bioactive molecules, such as proteins and pharmaceuticals. Therefore, it is important to analyze the internal structure with regards to pore size, homogeneity. Furthermore, diffusion of guest molecules and cells through the polymer network is of interest.[140] Scanning electron microscopy (SEM) and transmission electron microscopy (TEM) can be performed for detailed analysis of the morphology and microstructure of the microgels.[124,125] Using high resolution SEM (HRSEM) analysis, "outer" feature sizes down to the nanometer scale can be

Table 1. List of advantages and disadvantages of microgel characterization methods.

Characterization method	Size regime	Obtained measure	Advantages	Disadvantages
DLS/SLS[121–123]	10 nm to 5 µm	Hydrodynamic radius, size distribution, aggregates	Bulk analysis, polydispersity, in swollen/dispersed state	Refractive index contrast low in swollen state can be insufficient, no probing of individual microgels possible
TEM/HRTEM[124–126]	HRTEM: 1 Å	Morphology, homogeneity, chain dynamics	Information about morphology with very high resolution	2D image, imaging under vacuum → freeze-drying needed → might change structure, conductive layer is needed → might conceal morphology
Brillouin microscopy/refractive index tomography[118,120,127]	500 nm	Internal homogeneity, mechanical properties	Local structure elucidation inside microgel	Individual measurement
Real-time deformability cytometry[117,118]	≈15 µm	Mechanical properties	High-throughput method	Size limitation of microgels to max. ≈15 µm
Fluorescence microscopy[10,77]	Nanometer scale	Internal structure	Wide variety of applications using different fluorescent dyes/bioactive molecules	Fluorescent markers needed → might alter structure
FRAP/FCS[128–130]	Nanometer scale	Diffusion properties	For a wide variety of microgel sizes and shapes	Suitable models needed for evaluation
NMR[131–134]	Molecular scale	Chemical composition	Quantification of chemical groups, diffusivity of guest molecules	Sensitivity → Broad signals
AFM[135–137]	Nanometer to sub-nanometer scale	Mechanical properties, interaction forces	3D surface profile	Individual measurement

imaged.[125] TEM additionally gives information about the "inner" morphology of microgel with a resolution of up to 1 Å in high resolution transmission electron microscopy (HRTEM).[126] However, for SEM and TEM measurements the samples are imaged under vacuum, complicating imaging of the microgels in their native water-swollen state.[125] To address this issue, microgel samples are freeze-dried in an attempt to maintain the native structure in the absence of water. Water inside of the microgel is sublimated upon application of a strong vacuum, leading to the formation of a porous dehydrated polymer network. However, sublimation can also change the microgel structure, so the imaged structure might not always represent the original microgel state.[141] Additionally, for the characterization of microgels composed of dielectric polymer networks, a conductive layer is applied by sputtering a thin metal film (often Au or Pt/Pd) on top of the specimen, which might further conceal the real microgel morphology.

As an alternative, cryo-electron microscopy can be used for imaging microgel samples, for which freeze-drying is not suitable. In cryo-TEM the microgel structure can be imaged in its swollen form with almost atomic resolution.[142,143] The aqueous microgel sample is quickly frozen to liquid ethane temperatures, avoiding crystallization of water and leading to a vitrified state resembling the microgel structure in its native form. The vitrified sample can be microtomed and transferred to the TEM on a cooled sample holder.[125] No conductive coating is required due to the intrinsic electrical conductivity of the vitrified water.[125] During imaging, the frozen water can also be sublimated to reveal the naked microgel polymer slice.[142]

The advance of optical microscopy methods also allows imaging of microgels with down to almost molecular resolution. For example, the internal homogeneity of a microgel network and its mechanical properties can be characterized by confocal Brillouin microscopy combined with refractive index tomography.[118] Brillouin microscopy can be performed without any dye- or fluorescent label at high spatial resolution of around 500 nm. The method is therefore of interest for biological samples as well as for studying microgels.[120,127] Brillouin microscopy is based on inelastic scattering of incident photons on collective fluctuations of the molecules (acoustic phonons).[120] The measured Brillouin shift gives information about the longitudinal modulus, refractive index, and the absolute density of the sample.[118] On somewhat larger scales, optical imaging tomography (ODT) can be performed to gain information about the macroscopic homogeneity of the microgel network. Here, radial refractive index profiles are computed from representative phase images, allowing mapping of the internal structure.[118]

Confocal and super-resolution microscopy can be employed to gain 3D insight into the internal structure of microgels with resolution on the nanometer scale (see Figure 4d–k). However, for these techniques, the microgel network needs to be equipped with fluorescent markers, which might alter the structure of the microgels compared to a marker-free microgel of the same building blocks.[10,77]

Fluorescent markers also allow investigation of dynamic processes inside of the microgels. Fluorescence correlation spectroscopy (FCS) and fluorescence recovery after photobleaching (FRAP) are well-established methods to study structural and dynamical parameters of a microgel, accepting a wide variety of microgel sizes and shapes.[128,129] Small fluorescently labelled polymer chains (such as FITC-dextrans) or small molecular fluorescent dyes, are used for diffusion experiments inside the microgel samples. FCS measures the temporal fluctuation of fluorescence intensity. In FRAP, a spot in the fluorescent sample is rapidly

bleached and the recovery of fluorescence intensity in this spot is determined as bleached fluorophores diffuse out of the exposed spot and unbleached fluorophores diffuse in. Both techniques deliver diffusion coefficients for the respective microgel sample using suitable models.[129] Diffusion coefficients that are changing over time, suggests a more heterogeneous internal structure. FCS technique provides more accurate diffusion coefficients with better temporal resolution.[128,130]

Also, nuclear magnetic resonance (NMR) delivers information about diffusivity of guest molecules or the microgel network itself. Transverse relaxation in ^{1}H-NMR measurement deliver proton mobilities, enabling differentiation between specific areas in the microgels of for example the core and the periphery.[131–134] Furthermore, the phase transition of microgels between the swollen and the collapsed state can be followed precisely. Furthermore, the dynamics of solvent, and thus their diffusion coefficient, inside swollen microgels can be determined by diffusion ordered spectroscopy NMR (DOSY-NMR) and nuclear Overhauser enhancement spectroscopy (NOESY-NMR).[133,134]

4.3. Mechanical Properties

To obtain a first idea of the mechanical properties of a microgel, one can turn to rheological analysis of macroscopic bulk gels of the same polymer composition. Rheology on macroscopic gels is quick, sensitive, and requires relative small amounts of sample.[144] The rheological techniques, such as small amplitude oscillatory shear (SAOS) and linear viscoelasticity (LVE), allow for the determination of the storage and loss moduli, shear thinning properties, visco-elasticity, mechanical strength, etc.[144] This information can be used to estimate the mesh size and thus crosslinking density via the rubber elasticity or equilibrium swelling theory.[145] However, mechanical properties of small microgels may vary significantly from the macroscopic analysis, depending on the fabrication techniques that yield different and more or less homogeneous networks (see Figure 4).

To investigate the mechanical properties of individual microgels, colloidal probe nanoindentation and atomic force microscopy (AFM) have to be employed.[135,136] In colloidal probe AFM, a tip is modified with a micron-sized colloidal particle, with a diameter of up to 15 μm, which is used to deform and indent the microgel.[137,146] Bending of the cantilever during contact with the microgel is detected using a laser diode and a split photodetector, which gives information about tip-microgel displacement and the associated interaction force, thus allowing the calculation of Young's moduli for individual microgels.[137,147,148,149] Additionally, AFM can be used to measure the interaction forces between microgels with appropriate functionalities (biological recognition motifs or charges) with surface bound bioactive molecules, such as peptides and proteins as well as cells.[150,151]

Nanoindentation can be combined with fluorescence microscopy to analyze the correlation between mechanical properties and microgel functionalization or combine nanoindentation with Förster resonance energy transfer (FRET) measurements in a confocal microscope. These methods contribute to understand fundamental properties of functional microgels in biomedicine, such as molecular diffusion through the network and cellular interactions or uptake, depending on the microgel dimensions.

Colloidal probe nanoindentation is the most commonly used technique for analysis of mechanical properties of microgel but it is limited to measuring the elastic response at the particle surface and mainly has low throughput. Real-time deformability cytometry (RT-DC) was recently established as a high-throughput technique developed to analyze cell mechanical properties by measuring deformation under shear stress at laminar capillary flow conditions.[152] Besides the measurements of cells, cell-sized soft microgels can be analyzed with this technique as they can flow through a narrow microfluidic channel with a velocity of about 10 cm s^{-1}. The deformation of microgels as a response to the hydrodynamic strain induced by the flow in the channel allows to determine the elastic behavior and Young's moduli of the microgels at high throughput.[117,118]

5. Clinical Applications

Above, we have discussed how we can produce and characterize different microgels with precisely tuned properties. We have established that these variable and controllable properties render microgels ideal candidates for biomedical and eventually clinical applications.

Clinical application of microgels has first been suggested toward the end of the 1990s. Since then, microgels have evolved into a powerful class of materials for a variety of biomedical and therapeutic applications. In **Figure 5**, we draw a timeline to represent the most important developments in terms of microgel production methods with potential for clinical application. Of course, this timeline cannot be complete and we limit ourselves to what we see as the most influential works of the time.

In the following, we will discuss therapeutic microgels in further detail and discuss their potential for translation into the clinic. Here we focus on applications as drug delivery or toxin capturing vehicles, microgels as contrast agents carrying imaging probes, and microgels as building blocks for tissue regeneration scaffolds (see **Figure 6**).[153–155]

5.1. Therapeutic Microgels for Delivery and Capturing

Therapeutic microgel formulations can be administrated via different routes, such as oral, pulmonary, nasal, parenteral, intraocular, rectal, vaginal, or transdermal.[71,156,157] Depending on their chemical and physical properties, microgels can take up and deliver drugs of different polarity and charge.[71,156]

Different strategies for successful incorporation of drugs and active compounds into microgels have been pursued:

Covalent conjugation of bioactive molecules to microgels can be achieved during microgel synthesis or by post-functionalization.[41,115,157] While this mechanism provides high stability to the enclosed drug,[41] usually the drug has to be cleaved off and released from the polymer network to become active. For example, microgels were formed either in inverse microemulsion or dilute aqueous solution by copolymerization of acrylamide-based polymers with acrylic group modified enzymes as biological agents that can be released after hydrolysis.[158] In another approach, a carboxylate containing drug was bound to hydroxyl groups of polysaccharide-based microgels via ester

1998	Self-assembled hydrogel nanoparticle of cholesterol-bearing pullulan as a carrier of protein drugs: complexation and stabilization of insulin[303]
1999 - 2000	First Introduction of the term "Nanogel" to define swollen chemically crosslinked bifunctional networks of a polyion and a non-ionic polymer
2001	Hybrid poly(*N*-isopropylacrylamide)-based (polyNIPAM) microgels for sustainable thermosensitive drug release[304]
2004	PEG- and PEI-based microgels for oligonucleotide delivery across the blood-brain barrier[294]
2005	Direct fabrication and harvesting of monodisperse, shape-specific nanoparticles via PRINT that can contain therapeutic cargo for nanomedicine[305]
2005	New strategy for producing monodisperse solid microparticles with control over size, shape, and composition using microfluidics: production of polymer spheres, rods, disks, and ellipsoids[306]
2005	Controlled synthesis of monodisperse, non-spherical, plug- and disk-shaped microparticles using microfluidics[307]
2005	Novel microgel-quantum dot-hybrid nanoparticle for live cell imaging[308]
2006	Phase I clinical trial: HER2-specific T-cell immune responses in patients vaccinated with truncated HER2 protein complexed with microgels of cholesteryl pullulan[216]
2015	Phase IV clinical trial: Tretinoin microgel versus conventional bulk gel in patients with acne vulgaris: A randomized, active controlled, multicentre, parallel group[218]
2015	First report of microporous annealed particle (MAP) scaffold demonstrating enhanced cell infiltration *in vivo* for tissue engineering[87]
2017	First report of Anisogels using magneto-responsive, anisometric microgels to achieve aligned structures and oriented cell growth in surrounding hydrogel[309]
2019	First report of Microgel Scavengers sopping up toxins[77]

Figure 5. Timeline with important milestones.

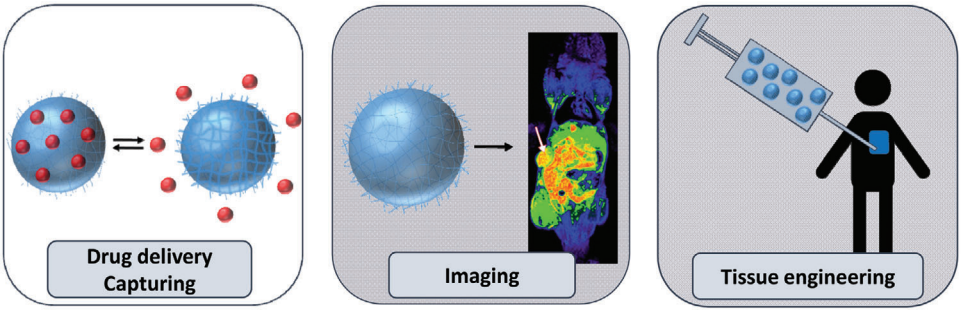

Figure 6. Drug delivery, imaging, and tissue engineering applications of microgels in biomedicine. Reproduced with permission.[249] Copyright 2018, American Chemical Society.

linkages. In the presence of esterase enzymes, the drug can be released.[41]

Noncovalent conjugation: Drugs can also be incorporated into microgels through noncovalent interactions, such as Coulomb attraction, hydrogen bonding, or hydrophobic interactions.[41] For drug loading of microgels using noncovalent conjugation to the cargo molecule, the microgel is swollen in a solution of the cargo and incubated to allow sufficient time for the guest molecules to diffuse into the microgel and interact with the respective supramolecular units. This often leads to relative low encapsulation efficiencies. If the interaction strength is sufficient, the microgels can be removed from the incubation solution (for example by centrifugation). Alternatively, the microgel can be collapsed (using a suitable trigger)—in this case, the cargo can only be released upon swelling of the microgel at the desired location.

The efficiency of drug entrapment and retention in the microgel network is determined mainly by the interaction strength, while diffusion out of the microgel depends on the size of the guest/drug molecule and the internal structure of the microgel.[115] Diffusion out of the microgel is important for covalently as well as for noncovalently bound cargo.

In therapeutic microgels, the drug-release is often characterized by a burst release and fast decay of the entrapped drug-molecules. This burst leads to high initial drug concentrations, which can be pharmacologically inefficient and dangerous due to concentration dependent toxicity of the drug or cargo molecule. Even a controlled burst release, with acceptable concentrations is often not desired as it requires frequent dosing. Especially drugs of low molar mass exhibit burst release profiles, due to their small size, high osmotic pressure inside of the microgel and fast diffusion through the microgel network.[159] Furthermore, the microgel size, porosity, and geometry, as well as microgel interactions with the environment can influence or prematurely trigger the burst release.[159]

Therefore, pharmaceutical research has focused on ways to avoid such burst releases. A successful pathway to avoid burst release in microgels is by employing a shell around the microgel to reduce the osmotic pressure gradient and facilitate a slower diffusion profile.[159,160] For example, a microgel with a crosslinked shell of ethylene glycol dimethacrylate (EGDMA) reduces the burst release to less than 10% of the initial loading capacity.[161] However, such modifications involve additional and often costly steps, which can sometimes result in reduced drug loading capacities.[159]

One successful example of a noncovalent drug immobilization strategy is through controlled self-assembly of polyelectrolytes.[41] Amphiphilic polymers spontaneously form microgels in aqueous media via self-aggregation mediated by intra- and intermolecular association. In the presence of hydrophobic molecules or aggregates, the self-aggregation leads to enclosure of the hydrophobic entities, reducing their interfacial energy while forming stable and robust microgel structures.[41,157] These participating molecules orient in such a way that the hydrophilic regions are exposed to the aqueous, polar environment and the hydrophobic segments are buried in the core of the microgels. In this case, it is possible to incorporate hydrophobic drugs, such as the anticancer drug doxorubicin (DOX) inside the microgels.

5.1.1. Stimuli-Responsive Microgels

Bioactive molecules can be retained in the microgels by interacting with specific ligands incorporated into the network. The binding strength of these interactions will affect the diffusion kinetics through the microgel. In addition to diffusive release, available in many swollen polymer-based delivery systems, a triggered release of an active compound or drug from the microgel can occur upon issuing different stimuli that are either biological, chemical, and/or physical in nature (see **Figure 7**).

Importantly, for stimuli-responsive microgels, swelling in an aqueous medium is essential as otherwise the drug molecule cannot be released from the microgel without degradation.[115] Drug release from microgels is always two-step process.

- First, the drug detaches from the network.
- Second, the drug diffuses out of the microgels.

During the second step, other attractive interactions between the network and the drug may take place slowing down the diffusion rate. Both steps can be induced and/or enhanced by specific triggers.[71,115,162] In the following, we will discuss different examples of such drug-releasing stimuli-responsive microgels.

Chemical Stimuli: Inside the body, different chemical signals can hamper the interactions between drug and microgel network. Biological fluids carry enzymes, proteins, and peptides as well as sugars and salts that may influence the swelling behavior, network stability, and degradation process. For example, pH-responsive microgels contain functional groups, such as carboxylic acid and amines or other acid/base type groups.[71,162] These groups gain charge upon protonation or deprotonation depending on the pH. This pH dependency entails also a change in the osmotic pressure, which can induce swelling and undesired release of an electrostatically bound drug.[71] As a result, for biomedical applications we need to design the microgel carrier with the biological environment of application in mind—for example, stomach, intestine, or in tumors.[71,163] Only then can we achieve controlled drug release at a specific physiological or pathological site.[164,165]

For example, pH-responsive microgels have been used to protect insulin from acidic degradation in the stomach, while release is enabled in the intestine, rendering microgel-protected insulin suitable for oral delivery.[166] Acrylic acid-based microgels retain a hydrophobic, collapsed state in the stomach due to protonation of carboxyl groups. After gastric passage, the increase of pH leads to swelling of microgels due to carboxyl ionization and hydrogen bond breakage.[166,167] In another approach, pH-responsive microgels were used to regulate the delivery and release of antitumor drugs for cancer treatment as tumor tissue exhibits a lower pH compared to normal tissue.[166] Here, methacrylated succinyl-chitosan (MASCS) copolymerized with diacrylamide containing ortho esters (OEAM) employed as acid-labile crosslinkers have been polymerized to form pH-responsive microgels.[168] Due to the ortho ester linkages, these microgels degrade at low pH and release DOX selectively in the tumor.[168] Alternatively, drug release can occur through displacement with counterions. For example, microgels based on poly(acrylic acid) (PAA)-polymer with negatively charged carboxyl groups have been used for encapsulation of proteins featuring positively charged amine

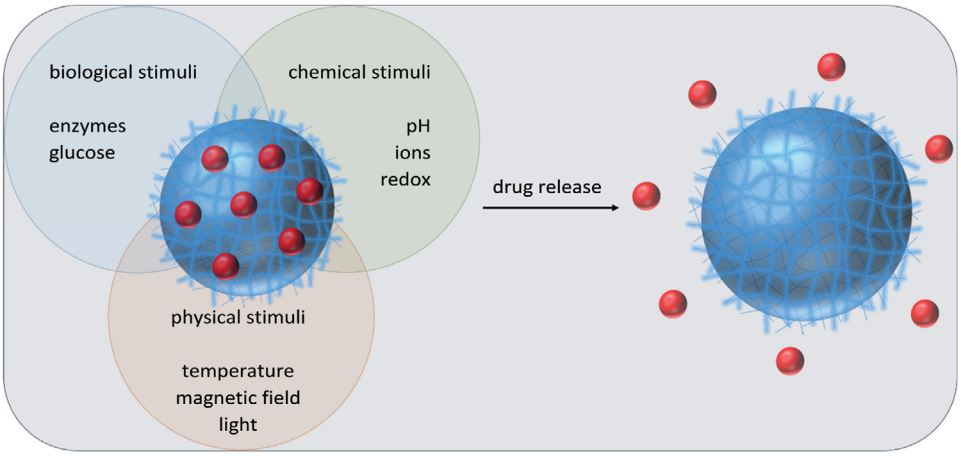

Figure 7. Drug release mechanisms of stimuli-responsive microgels.

groups. Protein release occurs via displacement of the proteins by adding positively charged ions, for example, calcium ions.[41]

Redox can also be used as a chemical trigger for release, which is of interest for clinical applications as pathological sites may produce of oxidative or reductive environments. Reduction-responsive microgels make use of the large difference in reductive potential between extra- and intracellular compartments to enable selective intracellular delivery of bioactive molecules, such as anti-cancer drugs, peptides, proteins, siRNA, and DNA.[162,169] The reductive potential between extra- and intracellular matrices is due to different concentrations of glutathione, ranging from 2 to 20 µM in body fluids, such as blood and extracellular matrices, to 0.5–3 mM in brain tumors[170], while its concentration inside cells is 2–10 mM[162]. For example, glutathione-degradable drug-loaded microgels can suppress hepatoma effectively and securely in a mouse model.[171]

In the second example, reduction-responsive methoxy-PEG-*co*-poly(L-phenylalanine-*co*-L-cysteine) microgels were synthesized via one-step ring-opening polymerization (ROP) of L-phenylalanine *N*-carboxyanhydride and L-cysteine *N*-carboxyanhydride with amino-terminated methoxy PEG as a macroinitiator. DOX was used as model drug. The microgels entered the tumor via the EPR effect,[172] where DOX was quickly released mediated by the high concentration of intracellular glutathione (GSH) (≈10.0 mM).[171]

In addition to pH and redox, enzyme-responsive microgels have great potential as drug delivery systems as enzymes like lipases, proteases, and glycosidases can recognize specific domains and induce highly selective bond scission.[162,173,174] For example, hyaluronic acid (HA)-based microgels have been copolymerized with di (ethylene glycol) diacrylate (DEGDA) for encapsulation of DOX.[175] The drug was loaded into the HA microgels through electrostatic interaction between the positively charged ammonium group of DOX and the negatively carboxylate groups of HA microgels, with a loading yield of 62%. The microgels were degraded by lipase and hyaluronidase, leading to drug release.[175]

Glucose-responsive microgels can be employed as a self-regulating drug delivery system for diabetes treatment (**Figure 8**).[162,163] A glycol chitosan (GC)/sodium alginate (SA)-poly(L-glutmate-*co*-*N*-3-L-glutamylphenylboronic acid) (PGGA) graft polymer microgel has been synthesized by an isotropic gelation and electrostatic interaction between GC and PGGA to form responsive microgels. The assembled microgels swell upon exposure to glucose, which is bound by incorporated boronic acid group on PGGA.[60] Swelling enables release of insulin. This approach resulted in controlled release of therapeutic doses of insulin at diabetic glucose levels over the course of 12 h.[60,163,176]

Physical Stimuli: If specific chemical triggers cannot be used to release active molecular cargo or degrade the microgel, physical triggers, such as body temperature, or external triggers, like light, and magnetic fields can be used to locally induce drug release.[177,178] Many polymers and microgels exhibit a cloud point (p_c) due to a lower- (LCST) or upper critical solution temperature (UCST).[71,163] Therefore temperature can be employed to switch the microgels between a swollen and a collapsed state.[71,179,180,181] LCST and UCST can be tuned by changing the hydrophilic or hydrophobic character of the microgel network.[177] Examples of polymers used to form microgels with an LCST are poly(diethylacrylamide), poly(*N*-isopropylacrylamide) (polyNIPAM), and poly(*N*-vinylcaprolactam) (pVCL).[177,181] When several of these polymers are employed together, microgels with multiple LCSTs—for example dual-temperature-responsive microgels—can be obtained.[182] To obtain microgels with a UCST, polymers need to be chosen that interact by hydrogen bonding as well as electrostatic interactions. Additionally, a certain degree of hydrophobicity should be present in the polymer to evoke favorable polymer-polymer interactions below the transition temperature.[180] Many UCST-type microgels are based on urea derivatives, such as poly(allyl urea) and poly(2-ureidoethyl methacrylate).[183,184] However, also other mixed polymer systems and composites can be utilized as UCST microgels.

Core–shell microgels consisting of polyNIPAM and zwitterionic sulfobetaine (SPB)-have been synthesized to exhibit combined UCST and LCST behavior.[185] For increasing temperatures from 4 to 25 °C, swelling of the poly-SPB shell with UCST was observed. Upon further increasing the temperature up to 50 °C, the polyNIPAM core of the microgel collapses due to its LCST.[185] It was shown that the respective critical temperatures could easily be tuned by changing the ratio and molecular weight of the con-

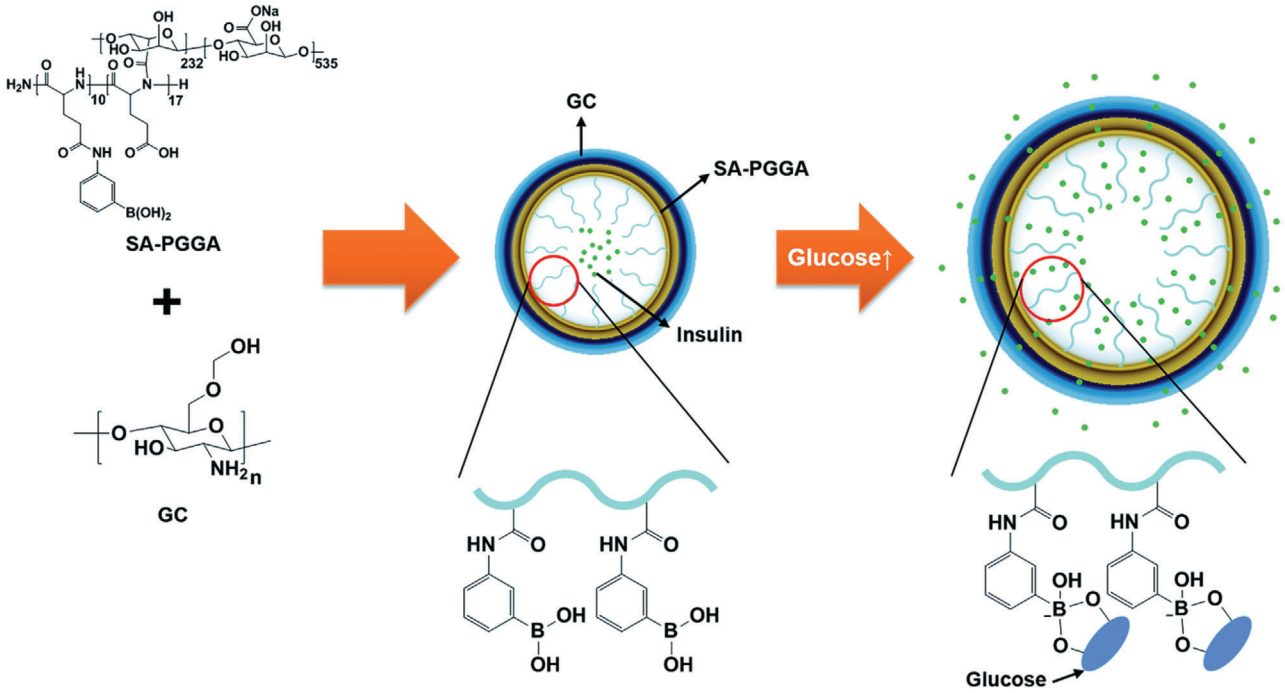

Figure 8. Schematic illustration of glucose-responsive GC/SA-PGGA double-layered microgel synthesis and insulin release by swelling of the microgels in the presence of glucose. Reproduced with permission.[60] Copyright 2015, Royal Society of Chemistry.

stituent polymers.[185] This core–shell microgel approach is particularly interesting for the delivery of therapeutic proteins due to the potency of poly-SPB to suppress protein aggregation.[186] Furthermore, this concept has been employed for biosensing and for the development of temperature-responsive scaffolds.[185]

To enable tunable elastic properties, core-shell microgels with a temperature-responsive polyNIPAM core and a nonresponsive poly(acrylamide) shell have been produced via droplet-based microfluidics.[187] The networks of the core and shells are covalently connected so that a collapse of the core at elevated temperatures lead also to stiffening of the shell.

For all thermos-responsive microgels, the presence of salts can greatly affect the LCST and UCST behavior of polymers and thus needs to be considered when designing microgels for medical applications.[185,188]

Light-responsive microgels are of interest for drug delivery, as an external light source can easily be focused on a specific area yielding site specific release. In principle, a variety of different wavelengths could be used and the exposure dose will impact the on-demand release kinetics of the drug.[177] However, for clinical applications, such light-triggered release is limited to wavelengths that can penetrate deep into tissue. Therefore, either wavelength of the tissue transparency windows in the near-infrared spectrum needs to be employed. Alternatively, one has to turn to very high doses to penetrate deep into the tissue; however, there remains a risk of tissue damage when operating outside of the transparency window.

Light-responsive microgels can either be obtained using photoactive organic moieties, such as reversible photoacids, photoswitches, photolabile linkers, or as hybrid systems with inorganic plasmonic nanoparticles.[177] Photoactive groups in the polymer can change the size and shape of the microgel by irradiation.[163] For example, a spiropyrane reversible photoacid turns into its charged merocyanine form upon exposure.[189] Azobenzenes inside of a microgel can change their conformation from *trans*-to-*cis* by UV irradiation, which leads to polarity changes inside of the microgel, triggering a change of the internal structure and potentially drug release.[163]

In the case of incorporated plasmonic nanoparticles, light is absorbed leading to local photothermal heating, which can swell or collapse UCST or LCST microgels, respectively. Beneficially, gold nanoparticles exhibit their plasmon absorption in the range of the tissue transparency window, rendering this type of IR light triggered UCST release suitable for clinical applications.[162,177]

Another way, to remotely induce microgel heating is by using magnetic field-responsive microgels, which are produced by incorporating magnetic nanoparticles, such as Fe_2O_3 and Fe_3O_4 nanoparticles into the microgel network.[162,163] Magnetic nanoparticles generate heat after exposure to an external alternating magnetic field (AMF), which leads to controlled drug release from temperature-responsive UCST microgels.[190,191] Additionally, the generated heat can also be used for localized hyperthermia treatment for cancer producing a therapeutic microgel for combined therapy.[162,163]

Several therapies combine different responsivities to achieve multi-functional and multi-responsive microgels.[162,163] For example, triple responsive photo-, pH-, and redox-responsive poly(acrylic acid-*co*-spiropyran methacrylate)-based microgels, crosslinked by disulphide-containing *N*,*N*-bis(acryloyl)cystamine, have been loaded with DOX via noncovalent interactions.[192] Drug release is achieved through breaking of the electrostatic interactions between amino groups of DOX

and acrylic acid groups of the microgels due to a local pH change in the tumor. Upon UV-light irradiation, the hydrophobic spiropyran in the microgels isomerized to the hydrophilic merocyanine leading to swelling of the microgels yielding faster release of DOX. Upon the addition of reducing agents, the polymeric network of the microgels degrades in smaller molecules due to oxidative bond scission of the disulfide crosslinkers and the degradation products can now be cleared more easily.[192]

In another combined example, pH-responsive microgels have been synthesized from photo-crosslinkable, biodegradable, and photoluminescent polymers (polyBPLPs).[193] BPLPs are low-molecular-weight aliphatic oligomers that include both water-soluble and water-insoluble oligomers that can be further crosslinked into polymer networks.[194] By the incorporation of different amino acids, such as L-cysteine into the polymer structure, strong and tunable autofluorescence with high photostability is generated to combine localization of tumor regions by fluorescence imaging and treatment via delivery of DOX.[194] For incorporation of DOX, PEG is copolymerized with the polyBPLP microgels. DOX is encapsulated inside the microgels via electrostatic interactions between DOX and the carboxylate groups of the microgel.[193] Drug release has been shown in vitro in acidic pH due to degradation of the ester linkages in the polymer network, displaying the potential for release in tumor environments.

In the third approach, dual pH/temperature-responsive hydrazide- and aldehyde-functionalized polyNIPAM-based self-assembled microgels were used for drug delivery to tumors.[195] The microgels has been tuned to exhibit a sharp swelling-deswelling transition over a temperature difference of only 2.2 °C above body temperature. This sensitivity to temperature enables controlled release in some tumors and inflamed tissue with increased temperature. In environment that are slightly more acidic the transition becomes even more steep.[28,196] Over time, these microgels degrade into low-molecular-weight species via hydrolysis of the hydrazone crosslinks.

5.1.2. Scavenging—Uptake of Radicals and Pathogens as a Strategy for Therapeutic Microgels

As a novel biomedical approach, microgels can be used as scavengers of molecules that are involved in diseases, such as bacterial infections or inflammatory disorders. Nitric oxide (NO), produced by nitric oxide synthase plays a key role in the human body, showing antibacterial, antitumor, vasodilation, and wound healing effects.[197] However, the overproduction of NO by physiological disorders can induce severe inflammatory diseases, such as rheumatoid arthritis (RA).[197] NO-scavenging microgels can provide a solution and are produced by solution polymerization of acrylamide with a NO-cleavable crosslinker (NOCCL) the treatment of RA.[197] When NO is exposed to NO-scavenging microgels, NOCCL is readily cleaved, consuming at the same time the NO molecule. The therapeutic efficacy in RA treatment has been tested in a mouse model in comparison to a commercial drug—Dexa—that is used in the clinic to suppress NO. Only NO-scavenging microgels could demonstrate long-lasting therapeutic effect until day 35, whereas free Dexa resulted in red and swollen paws after 14 days.[197] Dexa is a small molecule, which may be excreted more rapidly from the body compared to the higher molecular weight microgels, which could further explain the increased therapeutic effect of the microgels versus the free drug. However, possible toxic and side effects resulting from microgel application and their degradation products need to be investigated in further research before they can be transferred into a phase I clinical trial.

Reactive oxygen species (ROS), such as hydrogen peroxide (H_2O_2), hydroxyl radicals ($OH^{\bullet}$), and superoxide anions ($O_2^{\bullet -}$), are important signaling molecules in the human body, and necessary to maintain metabolism and cellular functions: such as cell proliferation, differentiation, signal transduction, pathogen defense, and regulation of inflammation.[198] An abnormal overproduction of ROS causes severe inflammatory diseases. Several antioxidants have been developed in the biomedical field to resolve high levels of ROS. However, high doses of natural antioxidants might also cause harmful effects on health, such as kidney stones, increased need for oxygen, excess uric acid excretion, and erosion of dental enamel.[199] To overcome this challenge, instead of using antioxidants, phenylboronic acid-tannic acid (TA) microgels as effective ROS scavenger are synthesized via self-assembly by simple mixing through to the formation of phenylboronic ester bonds between polymeric phenylboronate and TA (see **Figure 9**). Phenylboronic ester reacts with H_2O_2, while TA is a well-known antioxidant and specifically a free radical scavenger, consuming ROS radicals. TA-based microgels showed superior ROS scavenging capacity compared to natural antioxidants. Furthermore, the comparison of pure antioxidants to those incorporated in microgels show a significant reduction of inflammation using the microgels due to inherence of TA in the microgel polymer network.[198]

In another approach, PEG-based microgels, can be used as toxin scavengers. Toxin-mediated intestinal infections, such as cholera, shigellosis but also infection with *Clostridium difficile* (*C. diff.*) or pathogenic *Escherichia coli* (*E. coli*) strains result in secretory diarrhea and intestinal inflammation representing a major health threat in both the industrialized world as well as in developing countries.[77,200] So far, antibiotic treatment is applied to treat these infections. However, antibiotics do not eliminate the accumulated toxins, so a risk of relapse remains. To overcome this challenge for cholera, PEG-based microgels were functionalized with a glycosphingolipid receptor GM1a as scavengers for cholera toxin (CT).[77]

It could be shown that CT effectively binds to GM1a-functionalized microgels. GM1a-modified glycol-dendrimers and nanoparticles have been published as CT binding materials in previous reports.[201,202] However, these materials have small sizes and sterically restricted orientations of surface-grafted recognition motifs. Microgels have a larger size, preventing their cellular uptake by intestinal epithelial cells and contain a high degree of internal functionalization due to their meshed polymer network.[77] When HT-29 cells were exposed to CT and GM1a-functionalized microgels, CT had a higher affinity to the microgels compared to the surface receptors on epithelial cells and the HT-29 cells could be protected from the toxin.[77] Further research is needed to investigate the scavenging properties of microgels in vivo. However, functionalized microgels as scavengers have great potential to be an alternative to antibiotic treatment for several toxin-induced intestinal diseases.

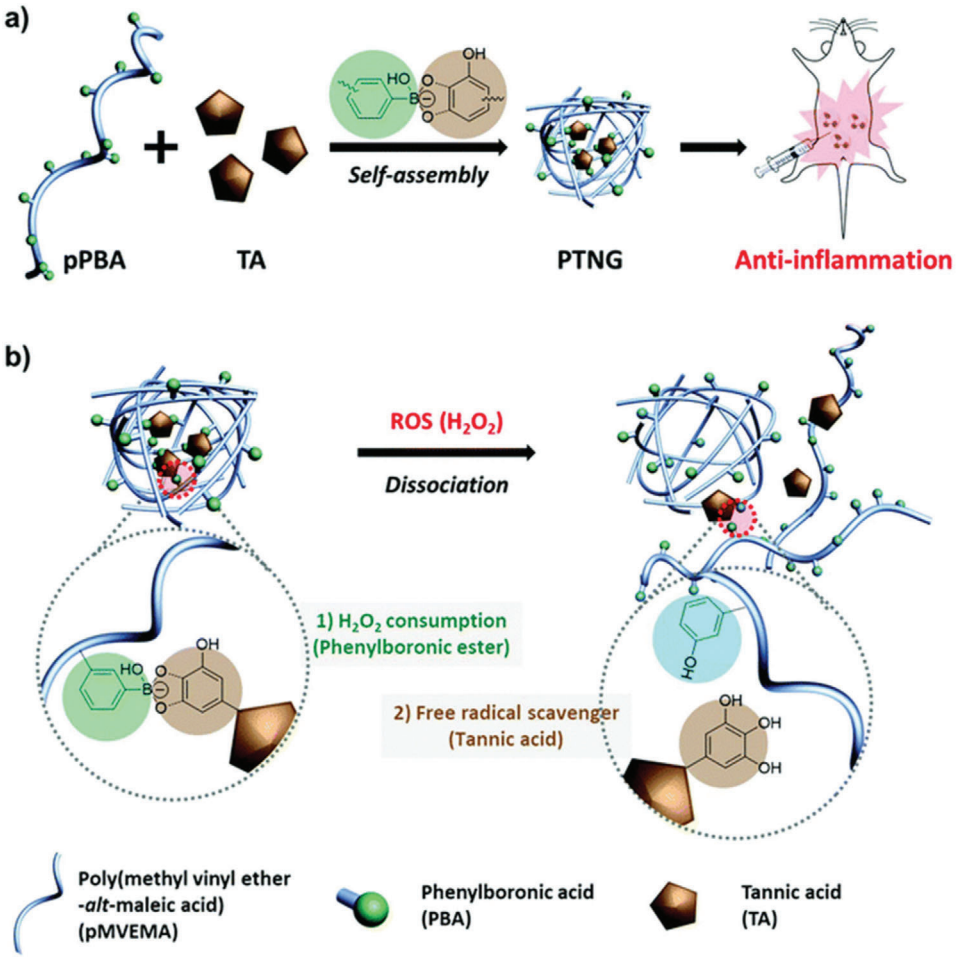

Figure 9. a) Preparation and administration of self-assembled phenylboronic acid-tannic acid microgels and b) illustration of ROS-scavenging capability of the microgels; the phenylboronic ester bond consumes H_2O_2 and TA scavenges the free radical. Reproduced with permission.[198] Copyright 2020, Royal Society of Chemistry.

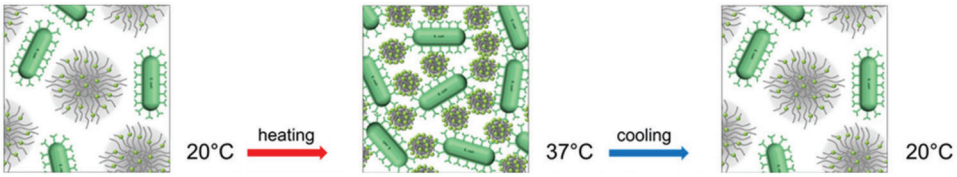

Figure 10. Schematic illustration of bacteria cluster formation in the presence of microgels above the LCST and release of bacteria below LCST. Scale bars, 10 µm. Reproduced with permission.[203] Copyright 2019, American Chemical Society.

Microgels have not only been used as scavengers for toxin but also to bind proteins and bacteria. For example, carbohydrate-functionalized temperature-responsive polyNIPAM microgels were produced for temperature-triggered capture of pathogens.[203] Microgels with a size range of 400–500 nm were synthesized via copolymerization of NIPAM with α-D-mannopyranoside (Man)- and β-D-galactopyranoside (Gal)-functionalized methacrylamide monomers at varying degrees of Man density and nonbinding Gal moieties. Man-functionalized microgels bind specifically to the concanavalin A (ConA) carbohydrate receptor, as well as to *E. coli* as a Man-binding model pathogen in a temperature-dependent manner (see **Figure 10**). Microgels with Man densities of 0.2–0.4% showed no clustering with ConA or *E. coli* below the LCST but showed mechanically stable clusters above the LCST of 37 °C of polyNIPAM. Improved binding above LCST was explained by reduced steric repulsion, smoothening of the microgel surface, and therefore enhanced accessibility of the Man groups. Microgels exhibit a strong increase in ligand density above the LCST since their volume decreases by an order of magnitude and hydrophilic binding motifs are phase separated and concentrated at the surface of the collapsed microgel.

5.1.3. TRANSLATION: Microgel Systems in Therapeutic Drug Delivery Application

While we have discussed the different fields of applications and the potential of therapeutic microgels, the following tables provide a concise overview on promising examples of microgels in preclinical (**Table 2**) and clinical (**Table 3**) studies:

From Tables 2 and 3, it becomes apparent that a variety of microgel systems have been developed with great success so that they are tested for clinical application in the body. We find examples where microgels improve the performance of local anesthetics, and where they are used as drug delivery systems for treatment of cancer, autoimmune diseases, neurodegenerative diseases, eye disorders, inflammation, diabetics, bone regeneration, as well as for transdermal drug- and vaccine delivery.[71] In the following, we will discuss exemplary cases where microgels have been tested in clinical trials. One of these is already clinically approved:

Example 1: Microgels based on rice powder with incorporated lidocaine hydrochloride (LH) and prilocaine hydrochloride (PH) were tested for anesthetic pain reduction in the human oral cavity.[215] The microgel system was developed as a delivery system to improve the adhesion to the mucosa in the oral cavity and therefore improve the local concentration and delivery efficiency of the anesthetic compared to previous available anesthetic bulk gels, creams, and ointments.[215,219]

Both types of microgels (with LH and PH) were tested in clinical efficacy studies with 100 healthy volunteers (25–60 years old). Pain measurements were evaluated after inserting a needle into the buccal mucosa after application of placebo microgels as negative control, commercial anesthetic gels as positive control, and anesthetic rice microgels containing 5% and 20% LH or PH.[215] Pain evaluation was performed using the visual analogue scale (VAS), numeric rating scale (NRS), and worst pain severity (WPS). The loaded microgels demonstrated pain reduction at both concentrations. The anesthetic microgels system is currently tested in patients with dental phobia in a phase I clinical study.

Example 2: Cholesteryl pullulan (CHP) microgels were complexed with 146HER2 protein to produce a CHP-HER2 vaccine for the treatment of patients with HER2 expressing tumors.[216]

Direct in vivo protein delivery approaches often suffer from poor stability, rapid proteolysis, and short half-lives of the active agent.[220] Here, hydrophobized amphiphilic polysaccharides, such as cholesterol group-bearing pullulan, were employed, which spontaneously form self-aggregated microgels in water through supramolecular host-guest interactions between host microgels that act as molecular chaperones and guest proteins.[221,222] On formation of the microgels, the pullulan orients in such a way that hydrophilic regions are exposed to the aqueous environment and the hydrophobic segments are buried in the core of the microgels. These microgels can trap non-native proteins, such as 146HER2 antigens that exhibit hydrophobic amino acid residues. The release mechanism is unclear; however, it is assumed that the HER2 antigens are released in the body by diffusion out of the microgels to interact with the immune cells and prepare them to attack the tumor.

In a phase I clinical trial, the safety and immune response to 146HER2 were evaluated in patients, which had cancer with HER2-expressing tumor cells. It was shown that the in vivo CHP-HER2 vaccine was successful. However, it was observed that five to nine vaccinations were necessary within a timeframe of 2.4 to 4.5 months to produce sufficiently high levels of HER2-specific $CD8^+$ T cells in peripheral blood. Unfortunately, this time frame is too long for cancer patients who need a rapid induction of immune responses.[216] Therefore, the required concentration of the 146HER2 protein to obtain an acceptable immune response is still under investigation.[216]

Nevertheless, this study shows a promising application of microgels in a vaccine antigen delivery system. The microgels enable facile formulation of stable vaccines. This project is a promising role model for the development of efficient cancer vaccines and potentially applicable to a variety of potent tumor antigens.[216]

Example 3: Tretinoin containing microgels were tested for the treatment of acne vulgaris in a phase IV clinical trial.[218] Tretinoin has shown effective therapeutic efficacy in the treatment of mild-moderate inflammatory lesions, such as acne vulgaris and has been the mainstay for comedolytic therapy.[223] However, due to the low water-solubility and instability of tretinoin in the presence of air, light, and heat, higher doses of the drug are required resulting in adverse effects such as erythema, dryness, peeling, and burning.[218] Microgels have been investigated to improve the surface area of the delivery vehicle compared to bulk gel, to increase the local concentration of tretinoin, while improving solubility and thus permeability through the pilosebaceous unit to effectively address acne vulgaris. Microgels, smaller than 200 nm were synthesized using an oil-in-water emulsion, while the lipophilic drug tretinoin was dissolved in oil phase and noncovalently incorporated into the microgel.

In the clinical phase IV study, patients of either sex between 18 and 65 years with acne vulgaris were treated transdermally with 0.025% w/w tretinoin containing microgels (Nioret Nanogel, Cadila Healthcare Ltd., India) and with conventional tretinoin gel (Retino-A Gel, Johnson & Johnson, India).[218] For approximately 50% of the patients, the microgel-tretinoin vehicle exhibited excellent efficacy, whereas only for 21% of the patients, treatment was rated nonefficient. Moreover, a significant reduction of inflammatory acne lesions was reported for the microgel formulation, compared to the conventional gel formulation.[218] An increased concentration of active drug can be applied using the microgel formulation, which improves clinical efficacy. However, 13.3% of the patients developed mild to severe adverse side-effects, such as dryness, skin irritation, and erythema. In conclusion, tretinoin containing microgels showed promising results in a phase IV clinical trial. The study was conducted in an open label design, where the probands see the label of the product. Despite the above mentioned side effects, tretinoin containing microgel showed superior performance compared to the previous gel formulation and the system is already approved and commercially available using different brand names for example Nioret (Nanogel, Cadila Healthcare Ltd., India) in India or Tretinoin Gel (Spear Pharmaceuticals, Inc., USA) in the United States.

In conclusion, therapeutic microgel systems have shown promising approaches for their application in drug delivery, as scavengers in several inflammatory disorders, or to capture and release specific pathogens or cells in the biomedical field. Microgels exhibit a high surface-to-volume ratio and can be loaded with

Table 2. Examples of microgels in preclinical trials and applications for drug delivery.

Application	Microgel material	Drug release trigger	Synthesis method of microgel	In vitro application	In vivo/Ex vivo application	Region	Ref.
Photothermal-chemotherapy of cancer using near-infrared light-triggered drug release based on host–guest associated microgels	(PPEGMA-*co*-PHPMA-*co*-PADMA)-PAMAM-CD microgels with encapsulated drugs	NIR light	RAFT polymerization	Release profiles	Intravenous injection of microgels; NIR-irradiation	China	[204]
Palliative treatment of advanced breast and endometrial carcinomas via oral delivery of megestrol acetate	Pluronic poly(acrylic acid) microgel	pH	Dispersion/emulsion polymerization	Release test; modelled conditions in the stomach (pH 1.8) and intestine (pH 6.8)	Microgel passage through rat intestine	USA	[205]
Oncolytic therapy via drug delivery (OA) from injectable microgels	PVA microgels with encapsulated oncolytic adenovirus (OA)	pH	Microfluidics	Release, infection, cytotoxicity study	In vivo: Lung tumor xenograft mouse model	China	[206]
Treatment of autoimmune diseases: systemic lupus erythematosus via microgel-based delivery of mycophenolic acid	Poly(lactic acid-*co*-ethylene glycol-*co*-lactic acid)-based microgels with encapsulated mycophenolic acid	n.a.	Photopolymerization	CD4 T cell binding tests	Autoimmunity study with mice	USA	[207]
Curcumin delivery from microgel for cutaneous wound repair	Curcumin encapsulated in polymeric micelles, loaded on hydrogel (Cur-M-H)	Temperature	Ring-opening polymerization	Release study of curcumin from microgel	Linear incision and full-thickness excision wound model in rats	China	[208]
Adjuvant-free intranasal vaccines for infectious diseases (influenza) via protein (antigen)-delivery from microgel	Cholesteryl-group-bearing pullulan (cCHP)-microgel with vaccine antigen	Protein-exchange mechanism	Self-assembly[209]		Intranasally administration to mice	Japan	[210]
Treatment of psoriasis via transdermal drug delivery from microgels	Acitretin and aloe-emodin loaded chitin microgels	pH	Regeneration of chitin: ion exchange of chitin and hydrogen bond interaction with drug	Release study of acitretin and aloe-emodin	Skin irritation study with mice	India	[211]
Treatment of diabetes via glucose-responsive insulin delivery from microgels	Glycol chitosan/sodium alginate-poly(L-glutmate-*co*-*N*-3-L-glutamylphenylboronic acid)-double-layered microgel	Microgel swelling in response to glucose concentration in the environment	*N* carboxyanhydride (NCA) polymerization	Insulin release study	Demonstration of controlled insulin release; retro-orbital injection of insulin-loaded microgels into mice	Republic of Korea	[60]
Release of cytostatic drug from microgels for imaging via MR	Alginate microgels containing holmium- and barium ions and liposomes	Temperature	Jet cutting method	Release test of fluorescein from microgels	Sheep kidney	EU (Netherlands)	[212]
Photodynamic therapy of skin cancer	Temoporfin (*m*-THPC) loaded microgel-peptide conjugates	Host–guest interaction; drug diffuses out over time	Thio-Michael nanoprecipitation method	Release study of *m*-THPC from microgel-peptide conjugate	Human skin penetration with *m*-THPC loaded microgels	EU (Germany)	[213]

Table 3. Microgels in clinical trials for drug delivery applications.

Application	Microgel material	Drug release trigger	Synthesis method of microgel	In vitro application	Clinical application	Region	Ref
Local anesthetics for pain reduction in human oral cavity	Rice powder-based microgel with incorporated lidocaine hydrochloride and prilocaine hydrochloride anesthetics	Degradation of the microgels	Dispersion polymerization[214]	Drug release study[214]	Microgel application in oral cavity	Thailand	[215]
Humoral immune response in patients with HER2-expressing tumors	Cholesteryl pullulan (CHP) microgels	n.a.	Spontaneous self-assembly of CHP in water[216]		CHP-HER2 vaccine injection in patients	Japan	[217]
Treatment of acne vulgaris via transdermal drug delivery from microgels	Tretinoin loaded microgels	n.a.	Oil-in-water emulsion		Treatment of the face	India	[218]

drugs and functionalized with any desired scavenging units, such as receptors, peptides, glycans, and ligands. Introduction of functional groups into the microgel can, therefore, lead to a larger extent of bound drug molecules or multivalent binding during targeting, compared to nanoparticles, polymers, and dendrimers. Furthermore, the swelling-deswelling property of microgels allows for stimuli-responsive control over drug and ligand binding affinity, while affecting diffusion through the network.

We have shown several promising examples of microgel systems which were transferred to preclinical and clinical trials. These trials mainly deal with therapeutic microgels for drug delivery application. However, only tretinoin containing microgels that are transdermally delivered have so far been approved in the clinic. In clinical trials of microgels via other administration routes such as oral, pulmonary, or nasal it is more difficult to fully understand their mechanism in the body and to prevent possible side effects. Unfortunately, the teams conducting the research about microgels based on rice powder with LH and PH for the anesthetic pain reduction in the human oral cavity (Example 1) and cholesteryl pullulan (CHP) microgels complexed with 146HER2 protein to produce a CHP-HER2 vaccine for the treatment of patients with HER2 expressing tumors (Example 2) did not respond to comment on any ongoing trials or planned product release.

5.2. Microgels for Imaging and Diagnostics

Imaging is an essential modality in the clinic to retrieve information about morphology, structure, and metabolism of pathogenic tissue for the identification and assessment of diseases.[13] The most commonly used imaging systems in hospitals and practices are computed tomography (CT), positron emission tomography (PET), magnetic resonance imaging (MRI), and optical or ultrasound (US) based imaging techniques.[13] Here, we will focus on these noninvasive imaging modalities in combination with microgels.

In many imaging techniques, the detected signal is generated by using contrast agents.[13] Most contrast agents that are clinically applied are based either on small molecules or on inorganic nanoparticles—but both are so small that they are rapidly cleared from the body, providing only a short temporal windows for imaging. Also, many agents are not specifically targeted toward pathological tissue, which often leads to reduced sensitivity and insufficient contrast.[13] Incorporation of contrast agents into microgels can help to overcome these challenges.[13,224] Microgels act as a cloak for the imaging probes to confer biocompatibility or solubility in biological liquids. Moreover, when the imaging probes are bound to the soluble microgel network, they are protected from aggregation and can unfold their full contrast potential. The controllable size and high colloidal stability of the microgels guarantee good circulation times together with high encapsulation capacity for a range of different contrast agents—especially for those lacking sufficient solubility in water. Likewise, the facile microgel modification with molecular contrast agents, as well as their functionalization with biomedical recognition motifs for targeting, are powerful tools to produce composite microgel systems for imaging application.[13] In contrast to drug-delivery systems, the cargo does not have to be released for contrast agents. Here, the focus lies on long circulation times, targeting, and the degradation or clearance of the carriers.

The development of hybrid microgels with combined stimuli-responsivity for controlled and targeted drug delivery and modification with contrast agents or incorporation of metallic imaging units allows for precise localization and treatment at the specific pathological site.[13] Such theranostic microgels combine therapeutic and diagnostic approaches and represent interesting candidates for advances treatment capabilities, where the pathological site and its extent is visualized, while drug delivery on-site can be monitored at the same time.[225] Such theranostic microgel systems for targeted cancer diagnosis and therapy have gained increasing attention in recent years.[226]

5.2.1. Magnetic Resonance Imaging

MRI is one of the most commonly used imaging techniques in the clinic due to several advantages, namely high anatomical resolution paired with high soft tissue contrast.[13] Two groups of contrast agents, affecting the spin-lattice or spin-spin relaxation times, T_1 and T_2 respectively, are used in this technique to enhance contrast.[13]

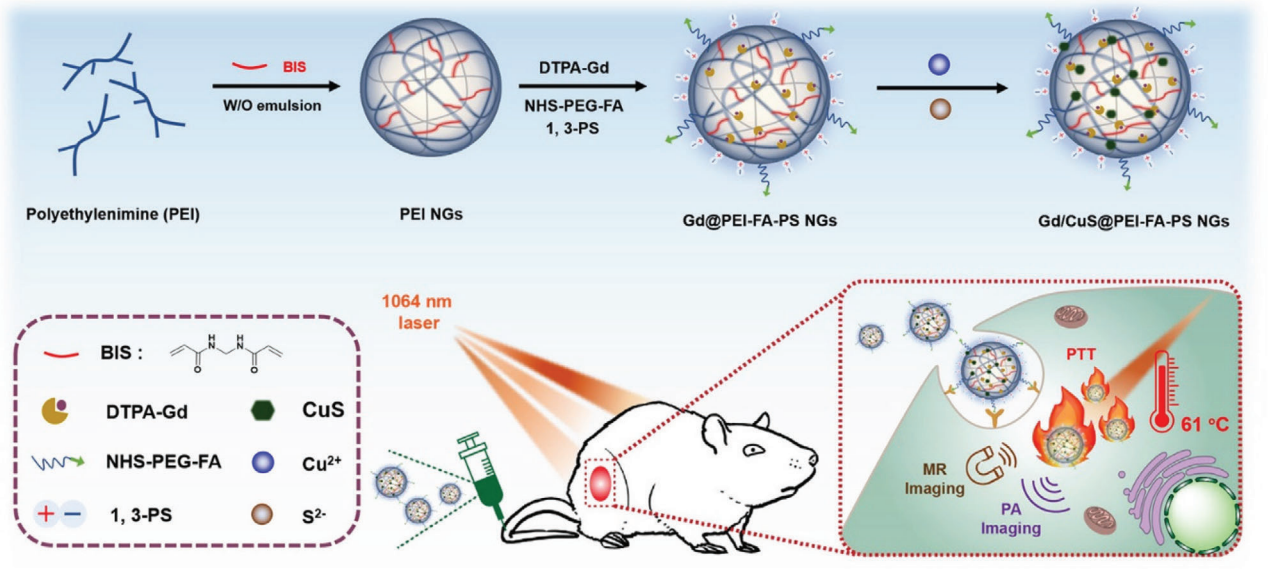

Figure 11. Schematic illustration of the preparation of Gd/CuS@PEI-FA-PS microgels for MRI/PAI-guided tumor-targeted PTT. Reproduced with permission.[229] Copyright 2020, American Chemical Society.

T_1 contrast agents are usually gadolinium (Gd) chelates.[13,227] They reduce the longitudinal relaxation time of the surrounding endogenous water, thus increasing the signal intensity and providing positive contrast. To further enhance contrast by augmenting Gd relaxivity, microgels can be used to encapsulate or conjugate the contrast agents. Poly(ethylene glycol) methyl ether methacrylate and *N*-(2-aminoethyl) methacrylamide hydrochloride were copolymerized to form microgels using ethylene glycol dimethacrylate as a crosslinker.[227] The pendant amine moieties were functionalized with an isocyanate derivate of diethylenetriaminepentaacetic acid (DTPA) to chelate Gd(III). The microgels showed enhanced spin-lattice relaxivity (shorter T_1) compared to linear polymers prepared under the same conditions in the absence of the crosslinking agents—but also an approximate fivefold enhancement in relaxivity in comparison to the clinically used contrast agent Gd(III)-DTPA (Magnevist) in in vivo studies.[227]

Many linear polymers are highly flexible, leading to more tumbling of the conjugated chelate in solution. Introducing a crosslinking agent and obtaining microgels, a higher rigidity is introduced in the polymer network leading to a better relaxivity. In MRI studies in mice, most of the microgel contrast agent remained in the vasculature for up to 7 days providing excellent long term contrast.[228] In comparison, Magnevist was mainly found in the kidneys and much less contrast was obtained in the targeted vasculature.[227]

The combination of imaging with therapy using multifunctional microgels opens promising approaches of theranostics in biomedical application. For example, Gd-/CuS-loaded functional microgels were used for MR/Photoacoustic (PA) dual mode image-guided tumor-targeted photothermal therapy (see **Figure 11**).[229] Poly(ethylene imine) (PEI) microgels were prepared by inverse emulsion method through crosslinking by Michael addition. The microgels were surface-functionalized with Gd(III) chelates and folic acid (FA) through a PEG spacer and 1,3-propanesultone. The FA in the microgels specifically target folic acid receptor (FAR), which is overexpressed in cancer cells. Cu(II) ions were loaded inside the microgels and subsequently reacted with S^{2-} to generate CuS nanoparticles in situ. The different compositions of Gd/CuS@PEI-FA-PS microgels enable admirable relaxivity (short T_1) and photothermal conversion efficiency due to the incorporated CuS nanoparticles with absorption in the second tissue transparency window.[229] The microgel system exhibit reduced T_1 and thus a more significant MRI contrast compared to individual CuS nanoparticles.[229,230] These approaches hold great promise for the development of microgel systems for image-guided therapy.

T_2 contrast agents are typically based on nontoxic superparamagnetic iron oxide nanoparticles (SPIONs), with different names that represent their size: very small vSPIONs and ultra-small uSPIONs.[13,178] However, the use of these contrast agents is limited because accumulation and aggregation of these agents can lead to negative contrast effects, making it difficult to identify lesions or other defects. Moreover, most superparamagnetic contrast agents incorporate water-insoluble Fe_3O_4 or γ-Fe_2O_3 with sizes between 4 to 180 nm.[13] Due to the small sizes, Fe_3O_4 is taken up by reticuloendothelial cells in the liver and spleen, which obviates their application in these areas for reasons of unknown toxic effects.[13] Microgels can be used to encapsulate iron oxide nanoparticles for example via hydrophobic interactions between the nanoparticles and hydrophobic pockets in microgels. Furthermore, clustering of iron oxide nanoparticles inside microgels allows them to work synergistically leading to enhanced T_2 relaxation times of water and thus a higher relaxivity. Also, the encapsulation of the iron oxide nanoparticles into microgels would most probably avoid their uptake in the liver and spleen, rendering such microgel SPION composites interesting for diagnosis in other organs, which could be targeted by attaching suitable biomedical recognition motifs.

The combination of MRI with other imaging modalities, such as fluorescence enables more precise disease localization and thus greater therapeutic efficacy.[13] For example, pH- and temperature-responsive microgels with dual MRI and fluorescence agents for medical imaging of brain glioma in rats were synthesized.[231] SPIONs were encapsulated in poly(NIPAM-*co*-AA) microgels, which were further modified with Cy5.5-labeled lactoferrin for fluorescence imaging and tumor targeting. In physiological conditions, the microgels were swollen. In the acidic tumor environment, the microgels collapsed, allowing them to accumulate in tumor tissue while improving local imaging contrast.

5.2.2. Positron Emission Tomography

PET is commonly used for molecular imaging in the clinic, especially in oncology, neurology, and cardiology.[13] This technique uses gamma rays emitted by radioactive tracers, enabling 3D imaging at unprecedented resolution and high sensitivity. Low concentrations of the imaging agent on the nanomolar scale are required for visualization.[13] As radioactive PET tracers, organic molecules with ^{18}F and ^{11}C are applied most commonly.[13] However, there are also studies, which use radionuclei with longer half-lives, such as ^{64}Cu, ^{86}Y, ^{89}Zr, and ^{68}Ga.[232] As is common to all small molecular imaging probes, uptake in the liver and spleen presents a problem and rapid clearance from the body due to their small sizes is challenging as it causes short temporal windows for imaging. To overcome these challenges, polymeric nanoparticles, micelles, and dendrimers have been developed as carrier systems.[13] However, problems with solubility and biocompatibility remain with these systems. By contrast, microgels exhibit excellent biocompatibility and enhance solubility of imaging agents in aqueous solution. Furthermore, microgels can be designed to exhibit stimuli-responsivity, which opens possibilities for disease-responsive imaging moieties. Furthermore, the combination of PET with MRI produces superior sensitivity and unmatched soft tissue resolution for anatomical imaging.[13] Dual-functional microgels containing chelates of both MRI and PET imaging agents can enable simultaneous faster imaging in clinical application in the future.

5.2.3. UV/Visible/NIR Optical and Photoacoustic Imaging

Optical imaging methods exhibit high sensitivity, nicely represented by the fact that this technique is regularly applied during image-guided surgeries to differentiate healthy from pathogenic or cancerous tissue.[13] Useful wavelengths for excitation and detection are in the range of the visible and near infrared (NIR) spectrum, depending on whether tissue needs to be penetrated (NIR) or not (visible).[233] Typical imaging agents are quantum dots, gold/silver nanoparticles, or fluorescent dyes with their respective excitation and emission wavelengths, photostabilities, quantum yields, and functional groups.[13,234] By contrast, photoacoustic imaging probes relax the photo-excited state thermally. Using a pulsed excitation source, the thermal relaxation can be picked up as ultrasound waves that show better tissue passage than light (NIR) waves.

The incorporation of the above mentioned dyes and particles in microgels enables targeted localization in the body. Furthermore, incorporation into microgels conveys improved solubility, superior in vivo stability, and optimized circulation times in the body, finally improving the contrast as more contrast agent can accumulate the site of interest.[13]

Quantum dots (QD) are nanocrystals typically composed of cadmium selenide (CdSe).[13] They exhibit unique properties, such as high resistance to photo-bleaching, high quantum yield, narrow emission spectra and the emission wavelength can be tuned by adjusting the size of the QD from the UV to the NIR spectrum.[13] QDs can be encapsulated inside microgels during synthesis facilitated by hydrophobic interactions between the hydrophobic QDs and hydrophobic pockets designed in the microgels.[235] Also, QDs can be formed in situ inside the microgels by adding CdSe-precursors to already prepared microgel precursor solution.[236] Furthermore, QDs can be prepared as core–shell particles, where a microgel shell is formed around individual CdSe QDs.[237] For example, core-shell QD-microgels were synthesized using hydrophobic CdSe-based nanoparticles.[237] CdSe nanoparticles as imaging probes are viewed with some criticism toward the biocompatibility since over long time Cd^{3+} ions are released from the QDs in biological fluids.[13] While microgels can cloak the QDs and make them more soluble, the microgel network is open enabling diffusion of ions and the increased size of the microgel compared to the QDs extends the circulation time, which is great for long term imaging; however, it remains problematic regarding the toxicity aspect and leaching Cd^{3+} ions. Therefore, as an alternative, carbon dots that are less toxic are investigated as alternatives for inorganic QDs.[238]

Another simple way of producing microgels for imaging is by incorporating fluorescent dyes.[239] The dyes can either be conjugated to the network after microgel formation or be incorporated in the microgel matrix during polymerization and crosslinking by modifying the fluorescent dyes with reactive groups.[13] This was done for example in a theranostic approach for cancer treatment, where reduction-responsive polypeptide microgels were synthesized using a polymerizable cyanine Br_2-IR808 dye.[240] The reduction-responsive microgels were used for drug delivery. Release was achieved by disassembly of the microgel structure, which could be visualized and monitored by means of the dye.

Alternatively, Au or Ag nanoparticles can also be used for imaging. While very small nanoparticles of such metals exhibit fluorescence, nanoparticles on the scale of ≈100 nm exhibit surface plasmons that can be excited by visible and NIR radiation. The major disadvantage of imaging at visible wavelengths is the limited tissue transparency at these wavelengths.[241]

In contrast to light detection, photoacoustic imaging (PAI) is a nonionizing imaging modality, where imaging probes are excited by light and the response is collected as pressure waves at ultrasound frequencies. Ultrasound waves are hardly scattered by tissue, providing deep tissue penetration compared to optical imaging and excellent spatial resolution and high optical contrast. PAI is therefore one of the most promising upcoming imaging modalities for disease diagnosis.[242] Since many diseases and physiological processes exhibit insufficient intrinsic PAI contrast, the use of extrinsic functional contrast agents is required.

PAI contrast agents are, for example, metallic nanoparticles, such as Au, Ag, QDs, CuS, iron oxide, and Pd, carbon

nanoparticles, or based of organic compounds such as polymer nanoparticles.[241] However, these contrast agents are generally nonbiodegradable and possess potential long-term toxicity and exhibit insufficient circulation lifetimes, which can be overcome using microgels as carriers. Microgels loaded with gold-nanoparticles (Au-NPs) as PAI contrast agents can be used for image-guided photothermally controlled drug release—and image-guided photothermal therapy (PTT) to destroy cancer cells without affecting surrounding healthy tissues.[242–245] The geometry and size of Au-NPs determine their photothermal efficiency. Thus, various Au-NPs geometries such as spheres, rods, cages, shells, and stars have already been described with respect to their potential as PAI probes.[243,246]

As is the case with many nanoparticles, the stability in biological fluids and circulation time are problematic. In plasmonics, nanoparticles aggregation can lead to plasmonic coupling between particles and a shift in the absorption wavelength, potentially diminishing the photoacoustic contrast as compared to the individual nanoparticle probes. Encapsulation of individual nanoparticles with a microgel shell provides a facile solution to these problems, facilitating photoacoustic imaging or even photothermal therapy.[247]

For example, polypeptide-Au-NP microgels were synthesized for targeted photoacoustic imaging.[248] Microgels were formed using two distinct triblock polypeptides via self-assembly and crosslinking of helical coiled-coil end domains. These microgels were loaded with the Au-NP by adding Au-precursor to the polypeptide mixture and nanoparticle formation and microgel formation proceeded simultaneously in situ. The obtained microgels showed good cytocompatibility, excellent cellular targeting, and high contrast photoacoustic imaging.[248]

Using temperature-sensitive polymer, such as polyNIPAM, as the microgel and loading it with Au-NPs and drug molecules, created image-guided and tumor targeting anticancer drug release vehicles. The polyNIPAM microgel can be collapsed by exposure to NIR light, facilitating the collapse of the polyNIPAM microgel when heated locally above its LCST. However, for drug delivery, a UCST microgel would be more suitable, as the drug could then be released upon triggering the swelling of the UCST gel.[245]

5.2.4. TRANSLATION: Microgel Systems in Therapeutic Imaging Application

To achieve precise and personalized therapeutic efficiency, diagnostic methods are in high demand for real-time monitoring of the therapeutic process.[226] In the following, diagnostic and theranostic microgel systems in preclinical trials are presented and their potential for application in patients is discussed (see **Table 4** for a list of applications and trials).

Of these promising examples of microgels used for imaging, we selected three examples to discuss them in more detail:

Example 1: Hybrid alginate (AG) and polyethylene imine microgels loaded with manganese oxide nanoparticles (AG/PEI-Mn_3O_4 microgels) were tested as MR agents for tumor imaging.[249] AG/PEI-Mn_3O_4 microgels show excellent colloidal stability in aqueous solution and good cytocompatibility.[249] AG/PEI-Mn_3O_4 microgels exhibit significantly enhanced MRI contrast, and prolonged imaging time compared to acetylated PEI.Ac-Mn_3O_4 nanoparticles used as a control (see **Figure 12**).[249] This enhancement is due to shorter T_1 relaxation time and extended blood circulation in mice. Moreover, the microgel system enables good biocompatibility in mice over the course of 30 days.[249]

A similar study was performed using alginate microgels with incorporated poly(ethylene imine) binding gold nanoparticles and Gd chelates (PEI-Au-Gd) for the formation of AG/PEI-Au-Gd microgels.[252] The AG/PEI-Au-Gd microgels were synthesized via double emulsion polymerization, while PEI-Au-Gd nanoparticles were used as crosslinker between the alginate carboxyl groups and the remaining PEI surface amine groups. PEI-Au-Gd nanoparticles and AG/PEI-Au-Gd microgels were compared in MR and CT imaging. AG/PEI-Au-Gd microgels are taken up by cells better than the nanoparticles alone and microgels also exhibit shorter T_1 relaxation times. These benefits lead to improved imaging performance of cancer cells in vitro and enhanced MRI/CT imaging of tumors in vivo compared to the PEI-Au-Gd nanoparticles. The microgels also surpass currently licensed contrast agents for clinical application in terms of contrast.[252]

Both studies successfully demonstrate the advantages and superior diagnostic performance of microgel systems compared to their analogous nanoparticle system for MRI and dual MRI/CT imaging. Both microgel systems show good biocompatibility in mice and are promising for MR and MR/CT imaging in humans for clinical application.

Example 2: Polyaniline (PANI)-loaded γ-polyglutamic acid (γ-PGA) microgels were used for PAI-guided tumor photothermal therapy.[242] γ-PGA microgels were first formed via double emulsification and crosslinked with cystamine dihydrochloride (Cys) via 1-ethyl-3-(3-(dimethylamino)propyl) carbodiimide hydrochloride (EDC) coupling chemistry. Aniline monomers were loaded inside the microgels via electrostatic interaction between the amine group of aniline and carboxyl groups of Cys-crosslinked γ-PGA microgels, followed by subsequent in situ polymerization in the presence of ammonium persulfate. The microgels showed good biocompatibility, cytocompatibility, and hemocompatibility. The γ-PGA/Cys@PANI microgels were used for PAI-guided PTT of xenografted tumor model of mice. The microgels showed strong PAI contrast and heat generation inside of the tumor under laser irradiation. To evaluate the PTT efficacy of the microgels in mice, the change in tumor volume was monitored over time. The injection of γ-PGA/Cys@PANI microgels plus NIR irradiation could induce tumor ablation, while only NIR laser irradiation or only administration of nanoparticles could not suppress tumor growth. These results show a promising example for the application of microgels as theranostics agents (combined photothermal imaging and PTT of tumors in vivo).

Example 3: Hybrid DOX loaded PEI-based microgels with incorporated uSPIONs were used for MRI-guided chemotherapy of tumors.[250] PEI microgels were synthesized with abundant amines via inverse mini-emulsion and surface post-functionalized with uSPIONs was achieved through 1-ethyl-3-(3-(dimethylamino)propyl) carbodiimide hydrochloride coupling. This system allowed for targeted tumor chemotherapy, releasing the anticancer drug DOX in response to the surrounding pH. The microgel system exhibits higher MRI contrast in comparison to corresponding free SPIONs.[250] Moreover, the microgels loaded with a DOX concentration of 2.5 μg mL^{-1} showed improved cell

Table 4. Examples of microgels in preclinical trials and applications for imaging.

Application	Microgel material	Incorporation of contrast agent	Synthesis method of microgel	In vitro application	In vivo/Ex vivo application	Region	Ref
MRI using alginate microgels loaded with manganese oxide nanoparticles	AG/PEI-Mn_3O_4 microgels	Chemical crosslinking of PEI–Mn_3O_4 NPs in AG microgels	Double emulsion	MR imaging of cancer cells was assessed	MR imaging of xenografted U87MG tumor-bearing mice	China	[249]
Microgels for photoacoustic (PA) image-guided photothermal therapy (PTT) of tumors	Polyaniline (PANI)-loaded γ-polyglutamic acid (γ-PGA) microgels	Aniline monomer is loaded inside γ-PGA/Cys microgels via an electrostatic interaction for subsequent in situ polymerization	Double emulsion	PAI-guided PTT of cancer cells	PAI-guided PTT of a xenografted tumor model (mice)	China	[242]
MRI/PAI-guided tumor-targeted photothermal therapy using Gd-/CuS-loaded functional microgels	PEI-based Gd/CuS@PEI-FA-PS microgels	Microgels were surface-functionalized with Gd(III) chelates; in-situ formation of CuS NP via reaction of Cu(II) ions with S^{2-}	W/O emulsion through Michael addition crosslinking reaction	Cytocompatibility of microgels is tested	MR imaging at KB-HFAR or KB-LFAR tumor-bearing nude mice	China	[229]
MRI-guided chemotherapy of tumors via cancer drug delivery from microgels	Fe_3O_4/PEI-Ac microgels	Microgels were covalently conjugated with citric acid-stabilized Fe_3O_4 NPs through (EDC) coupling and physical encapsulation of DOX	Inverse mini-emulsion polymerization	Cytocompatibility of drug-free microgels is assessed	Fe_3O_4/PEI-Ac microgel/DOX complexes are used as contrast agent for MR imaging in mice	China	[250]
CT imaging	γ-PGA–[(Au0)200 –PEI·NH2–mPEG] microgels	In situ chemically crosslinking of microgels with PEI-entrapped Au NPs	Double emulsion	Cytocompatibility, cellular uptake test and CT imaging of cancer cells	CT imaging of xenografted HeLa tumor model	China	[14]

(*Continued*)

Table 4. (Continued).

Application	Microgel material	Incorporation of contrast agent	Synthesis method of microgel	In vitro application	In vivo/Ex vivo application	Region	Ref
Multifunctional MR/fluorescence imaging agent for glioma diagnosis using injectable pH/sensitive magnetic microgels	Cy5.5-lactoferrin-poly(*N*-isopropylacrylamide-*co*-acrylic acid) microgels	Coupling of Cy5.5-Lf to microgels via coupling reagents (EDC HCl and Sulfo-NHS)	Emulsion polymerization	Rat C6 glioma (C6) cells, human umbilical vein endothelial cells	Rats gliomas treated with microgels	China	[231]
X-ray computed tomography imaging and chemotherapy of breast tumors via intratumoral or intraveneous injection of microgels	Hyaluronic acid-iodixanol microgels	n.a.		Drug release study from HAI-microgels	Microgel injection in tail vein of mice	China	[251]
US and T2-weighted MRI using dual-enzyme-loaded multifunctional hybrid microgels	SPIO@GCS/acryl/biotin-CAT/SOD-microgel	Hydrophilic/hydrophobic interactions and electrostatic attraction between the monomer and the SPIO particles and dual enzymes followed by mild enzymatic polymerization	Enzymatic polymerization		Intratumoral or intravenous injection, US- and T2-imaging of rabbits bearing VX2 tumors	China	[178]
MR/CT imaging using PEI-Au-Gd nanoparticles crosslinked in alginate (AG) microgels	AG/PEI-Au-Gd microgels	Chemical crosslinking of PEI-Au-Gd NPs in AG microgels	Double emulsion	Cytocompatibility, cellular uptake assay, MR/CT imaging of microgels	Biodistribution of microgels in mice	China	[252]
Imaging, biodistribution analysis using NIR-labeled microgels	p(OEGMA-*co*- PDSMA-*co*-Cy7)-microgels	Covalently bound Cy7 NHS ester to polymer structure of microgels	RAFT polymerization		Whole body fluorescence measurement of mice; ex vivo investigation of liver, spleen, intestine, lung, heart, kidney	USA	[253]

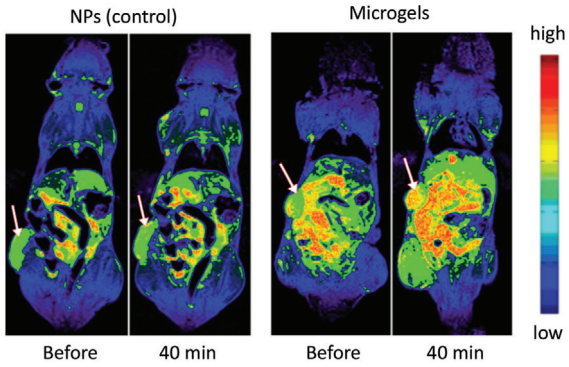

Figure 12. In vivo color T_1-weighted MR images of xenografted U87MG tumor-bearing mice before and after 40 min postintravenous injection of the AG/PEI-Mn_3O_4 microgels. Arrows indicate the tumor regions. Reproduced with permission.[249] Copyright 2018, American Chemical Society.

viability compared to DOX-loaded SPIONs with a concentration of 1 µg mL^{-1}.[250,254] As such, DOX-loaded SPION functionalized microgels represent a promising approach for MRI-guided chemotherapy.

Imaging is an essential tool for diagnosis of diseases, such as cancer, inflammation and other diseases that possess pathological tissues to be imaged. Many contrast agents that have progressed into clinical applications still suffer from several drawbacks, such as rapid clearance from the body and unspecific binding toward pathological tissue. It has been shown that incorporating these contrast agents inside microgels can help to overcome these challenges.

In general, microgels showed enhanced imaging contrast compared to the individual free imaging units—and clinical agents. Moreover, microgels as carrier for imaging units increased their water-solubility and thus biocompatibility and cytotoxicity.

However, it has to be clarified whether the microgels and the imaging unit can be degraded in and be cleared from the body. If microgel degradation is desired after imaging, it is essential to find ways to prevent potentially toxic side products of the gel and the contrast agent. To transfer further microgel systems to clinical trials in humans, it will be crucial to find answers to these questions.

5.3. Microgels as Scaffolds for Tissue Regeneration

For tissue regeneration, 3D constructs are often required, while for soft and sensitive tissues, a minimal invasive approach should be taken to avoid further damage.[4,5] In contrast to established hard implantable scaffolds, injectable liquid materials do not require a surgical excision to make space for the scaffold but instead they adjust to irregular shapes and cavities. To produce such a liquid scaffold precursor, one needs precise control over the polymerization and crosslinking reactions. These reactions need to take place under physiological conditions to fill the respective void completely and form the adapted construct while achieving an intimate contact to the surrounding tissue.[255,256] Several injectable hydrogel systems have been developed for the treatment of cartilage, intervertebral discs, bone, adipose tissue, spinal cord, brain, heart, and muscle injuries.[256] However, such injectable molecular precursors crosslink into isotropic nanoporous hydrogels, limiting endogenous cell infiltration and do not provide directional guidance for the cells. This guidance is crucial for the reconstruction of many structured tissues. Some approaches to achieve hydrogels with larger micron-scale pores after injection have been presented but still lack defined porosity or they leach nonpolymerized monomers or porogen material with unforeseeable adverse side effects that might only become apparent at later stages.[257–260] Moreover, injectable hydrogel materials for tissue regeneration must precisely match the rate of degradation to enable tissue development; too rapid degradation lead to insufficient scaffolding, while a rate that is too slow will prevent proper tissue development and will promote fibrosis.[87] The degradation rates can be adjusted using hydrolytically and enzymatically degradable moiety and crosslinkers. However, every tissue site has unique physical and chemical requirements for functional tissue regeneration, demanding a material strategy that is versatile and applicable for a variety of challenging cellular environments. To overcome the need for material degradation prior to tissue ingrowth, a new class of injectable biomaterials has been developed. This class is termed microporous annealed particle (MAP) scaffolds[87] and microgels have proven powerful building blocks to intercrosslink and form MAP scaffolds.[261–269] Microgel-based MAP scaffolds can have different interstitial pore sizes by changing the microgel diameter.[270,271] These micron-scale interstitial pores facilitate cell infiltration, as the cells do not need to degrade the material to create an open path. The internal network structure of the microgel building blocks mediates softness and can present biomolecular cues, such as growth factors. The concept of MAP scaffolds combines injectability and microporosity for efficient cellular network formation, bulk tissue integration, and regeneration in vivo.[87,263,265,266,268,272] It was shown that the MAP scaffold properties, such as microgel size, void space, stiffness of microgels, cell adhesion ligand concentration and presentation, as well as modular block size of the scaffold can modulate cell spreading, proliferation, and nonviral gene transfer to cells cultured with scaffold.[264,269,273] These findings reveal that the properties of MAP scaffolds can be altered on demand for biomedical applications. There are currently several promising publications of MAP scaffolds used in tissue regeneration applications.[87,263,265,268,272,274,275] For example, an injectable and adaptable microporous hydrogel was formed by the assembly of two oppositely charged microgels.[268] Thereby, gelatin-methacryloyl (GelMA) microgels containing negatively charged carboxy groups and chitosan oligomer methacrylate (ChitoMA) microgels containing positively charged amino groups interacted with each other. MAP hydrogels with suitable micropores provide mechanical support for rapid cell migration and transport of bioresponsive cues to direct cell adhesion and growth. The incorporation of growth factors into the building blocks, combined with the cell-penetrative connected pores constructed by the MAP scaffold inside a nerve conduit, effectively showed Schwann cell (SC) migration and induced dramatic bridging effects of peripheral nerve defects by accelerated axon outgrowth.[268] In another approach, MAP scaffolds were used for wound repair by immunomodulation.[275,276] PEG-based microgels were produced via inverse suspension polymerization

and loaded with human mesenchymal stem cells (hMSCs) before MAP scaffolds were formed.[276]. It is known that hMSCs have the unique ability to shift macrophage polarization from an activated pro-inflammatory M1 phenotype to a deactivated anti-inflammatory M2 phenotype. In this study, hMSC-laden MAP scaffolds were cultured in the presence of prepolarized M1 macrophages and found to limit activation to the M1 phenotype, even in the presence of pro-inflammatory cytokines such as TNFα.

In contrast to spherical microgels that form densely packed colloidal glasses, rod-shaped microgels with higher aspect ratios can be jammed, resulting in larger pores and the possibility to convey directionality.[10] These 3D constructs permit cell interaction with the microgels, while providing sufficient space for ingrowth of more cells and potential formation of blood vessels to support tissue maturation.

To obtain directional hydrogel structures with defined guiding elements after injection, magneto-responsive anisometric microgels were mixed inside a hydrogel precursor solution, forming a so called Anisogel.[102] The Anisogel microgels are based on PEG and prepared by in-mold PRINT polymerization. Once injected, a magnetic field is applied to align the rod-shaped microgels, providing directionality inside the final Anisogel with a common director, along the magnetic field. For this alignment, the field can be as low as a few mT (millitesla)—and the orientation is fixed by the surrounding crosslinking hydrogel precursor, which enables removal of the magnetic field.[277] When mixed with cells or neurons, the cells align and grow parallel to the aligned rods. As the fibronectin produced by the oriented fibroblasts is also oriented, this provides a positive feedback cycle as the natural oriented ECM can replace the degrading Anisogel and thus maintain the previously induced directionality.[80] This technology fills a gap between existing implantable anisotropic scaffolds and injectable isotropic materials.

A comparative study with variable microgel dimensions, aspect ratios, and distances revealed that microgels with a length of 50 μm and a width of 2.5 μm significantly enhanced neurite growth without jeopardizing cell alignment. By contrast, 5 μm wide microgels likely inhibit some axonal growth due to the larger cross-sections. Importantly, when the width was reduced to half, the distance between microgels had to be reduced from 34 to 24 μm to maintain unidirectional neurite extension; in fact, it reduced the volume fraction of microgels from 1 vol% to 0.45 vol%, producing an very infiltratable Anisogel scaffold for cells.[278,279,280]

Besides functioning as building blocks of injectable regenerative scaffolds, microgels can function also as individual containers to transplant cells or produce cell laden scaffolds in vivo.[84,281] Cell transplantation promises advanced therapy for stroke, spinal cord injury, and organ vascularization and regeneration.[282–284] However, in current systems only a small fraction of the cells are functional and remain at the target site, resulting in high cost and low efficiency. Here, the microgels can offer a solution by providing mechanical, physical, and biochemical stimuli to the cells, while they enhance the local retention at the site of injection in the body, and protect the cells from immune attacks. By coating the cells with different ECM proteins via layer-by-layer deposition, their viability inside the microgels can be further enhanced. Microgel encapsulated with a co-culture of human fibroblasts and cardiomyocytes derived from pluripotent stem cells demonstrated a native like heartbeat.[281]

5.3.1. TRANSLATION: Microgel Systems in Therapeutic Tissue Engineering Application

While we have discussed the potential of microgels in tissue engineering application, we now focus on promising examples of microgel systems in preclinical trials (**Table 5**).

From Table 5, it becomes apparent, that there are various therapeutic microgel systems that have been explored in preclinical studies for different applications in tissue engineering. Microgels have been explored for enhancing angiogenesis, heart repair, and wound healing. Among these promising examples we selected three microgel systems that we discuss in more detail:

Example 1: Stem cell transplantation is a promising approach for tissue repair. Multiple stem cell systems have already entered the stage of clinical testing.[286] However, the efficacy of clinically implemented stem cell treatments is limited by low retention and insufficient engraftment of transplanted cells at the site of injection. Furthermore, there is a potential risk of inflammation and immune reactions when allogeneic or xenogeneic cells are used.[286] To circumvent these problems, human cardiac stem cells (hCSCs) were encapsulated in temperature-sensitive poly(*N*-isopropylacrylamine-*co*-acrylic acid) (poly(NIPAM-AA)) microgels and the system was tested for treatment of acute myocardial infarction in a preclinical pig model.[286] The microgels were able to promote stem cell proliferation and clustering, while the swollen network of the microgels supports transport of nutrients, oxygen, and diffusion of regenerative factors secreted by the encapsulated cells. As the cells are mechanically protected from the outside, cell function and survival are maintained.[286] After injection, the microgel-encapsulated human CSCs promoted cardiac function and angiomyogenesis in the post-myocardial infarcted pig heart.[286] However, there remain some challenges, which need to be overcome before moving on to human trials. For example, in mouse and pig models, a permanent vessel ligation was applied, which is not performed in the clinic, as instead, patients normally get coronary reperfusion.[286]

Example 2: MAP scaffolds were produced from PEG-based microgels building blocks produced via microfluidics. The microgels were crosslinked with L- or D-chirality peptides for regenerative wound healing.[272] In comparison to wounds in the absence of MAP leading to loss of tissue, L- or D-MAP microgel scaffolds filled the wound defect and epidermis was formed over the scaffold. Changing the chirality of the interlinking peptides from L- to D-amino acids showed slower enzymatic degradation in vitro. Moreover, MAP scaffolds interlinked by D-peptides, led to activation of the adaptive immune system over time, resulting in significant tissue regeneration and healed cutaneous wounds including hair neogenesis.

Example 3: Injectable multi-functional RGD-conjugated alginate-based microgels have been used for delivery of both cells and growth factors to induce in vivo neovascularization.[285] The microgels were loaded with outgrowth endothelial cells (OECs) and the cells exhibited excellent cell viability inside the microgels.[285] The injection of RGD-microgels containing OECs into a hindlimb ischemic mouse model increased angiogenesis

Table 5. Examples of microgels in preclinical trials and applications for tissue regeneration.

Application	Microgel material	Therapeutic functionality	Synthesis method of microgel	In vitro application	In vivo/Ex vivo application	Region	Ref
Regenerative wound healing using MAP scaffolds	PEG-based microgels were pelleted to MAP scaffolds	Slow MAP degradation by switch of chirality of crosslinking peptides	Microfluidics	MAP degradation	Mouse excisional wound healing model	USA	[272]
Enhanced neovascularization using injectable multifunctional microgels	RGD-alginate-based microgels with encapsulated OEC cells	Cell encapsulation	Electrospraying	Long-term release of encapsulated materials	Hindlimb ischemia mouse model	South Korea	[285]
Heart repair (MI) using microgel-encapsulated HCS cells	P(NIPAM-AA) microgels with encapsulated HCS cells	Cell encapsulation	Emulsion polymerization		Ex vivo study with mouse and pig hearts	USA	[286]
Bone repair and regeneration using ECM-like microgels	Injectable nanofibrous heparin-modified gelatin microgels	Switch of proinflammatory macrophage into prohealing phenotype by polarization via sustained interleukin 4 (IL4) release	Emulsion polymerization	Bioactivity assay of IL4 release	Rat mandibular periodontal fenestration model	China	275
Treating Myocardial Infarction using injectable drug-releasing MAP scaffolds	Drug loaded PLGA/PEG-based NP are encapsulated in PEG-based microgels and form MAP scaffolds	Injection of drug releasing drugMAP hydrogel	Microfluidics	Drug effects on cardiomyocytes	Ischemia-reperfusion MI model and intramyocardial injection of drug MAP	USA	[265]
Wound healing on corneal epithelium using micronized sacchachitin-based microgels	Micronized sacchachitin (mSC)-based microgel	Microgels		Cell proliferation study	Rabbit corneas	China	[287]

(*Continued*)

Table 5. (Continued).

Application	Microgel material	Therapeutic functionality	Synthesis method of microgel	In vitro application	In vivo/Ex vivo application	Region	Ref
Tissue regeneration using injectable and orientable magneto-responsive soft anisotropic microgels	sPEG-A, PEG-DA-based microgels with SPION (EMG700, Ferrotec)	SPIONS are physically entrapped inside the polymer network	PRINT		Microgel injection in the lumbar region of the mouse spinal cord	EU (Germany)	[277]
Enhanced tissue vascularization using microgels with encapsulated hMSC	hMSC embedded Collagen-based 4S-star-PEG microgels	Cell encapsulation	Thermal crosslinking of polymer droplets on a hydrophobic surface		Hindlimb ischemia mouse model	Ireland	[288]
Tissue engineering and regenerative medicine application via cell delivery using microgels	Alginate-based microgels with singly encapsulated mMSC and hMSC cells	Microfluidic cell encapsulation	Microfluidics	Cell culture experiments	Mouse model, biodistribution of mMSC with and without microgel encapsulation	USA	[86]
Tissue regeneration and delivery of therapeutics using an injectable composite hydrogel/microgel system	Bulk host–guest hydrogel/microgel-system with IL-10	Injectable hydrogels are produced via host-guest crosslinking and combined with microgels with encapsulated drug	Microfluidics		Rat myocardial infarction model, injection of IL-10 containing hydrogel/microgel composite into the border zone region of the infarct	USA	[22]
Heart tissue regeneration: Myocardial infarction using injectable microgels with encapsulated cells	Reduced graphene oxide (rGO)/alginate microgel with encapsulated MSC	Cell encapsulation	Electrospraying	Cell culture experiments	Myocardial infarction model in rats	Republic of Korea	[85]

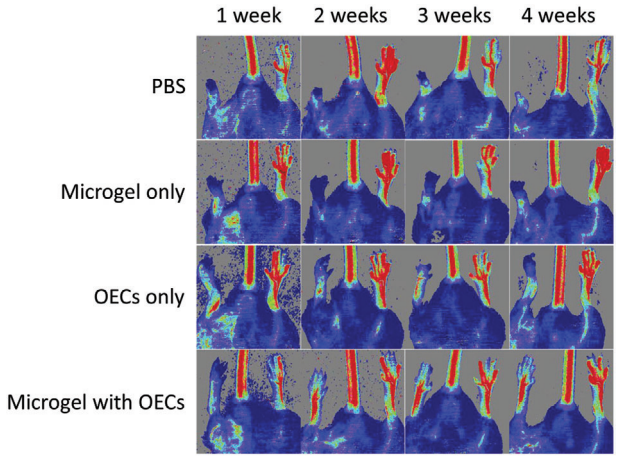

Figure 13. The recovery of blood flow perfusion of the ischemic hindlimb of mice, treated with PBS, empty RGD-alginate microgels, free OECs, and OECs-laden RGD-alginate microgels. After treatment, blood perfusion to the hindlimb was evaluated using a laser-Doppler flowmeter every week for 4 weeks. Reproduced with permission.[285] Copyright 2014, Elsevier.

and improved blood flow perfusion in comparison to individual OECs and empty microgels (see **Figure 13**).[285] In this study, the cell-laden microgels were compared to an analogous bulk hydrogel system, which the injectable microgel system outperformed with superior biocompatibility as well as reduced cytotoxicity (**Figure 14**).

In conclusion, injectable, interlinkable, and alignable microgel composites can pave the way for minimal invasive microgel therapies with or without therapeutic cells to regenerate sensitive and complex tissues, such as heart tissue after myocardial infarction or nerve tissue after spinal cord lesions. The use of microgels to form hierarchical and structured regenerative materials was recently part of a comprehensive review paper.[289]

These microgels cannot only function as scaffold but also support cellular therapies, which will play a more important role in the treatment of cancer, cardiac diseases, and tissue regeneration in the future. However, cell-laden microgels have only been tested in preclinical trials, using mice, rabbit, and pig models. In contrast to microgels, bulk hydrogel systems for tissue engineering and regenerative medicine applications are already undergoing clinical trials[290] as the use of microgels in this field is a more recent development. However, considering the named benefits of microgels, they have great potential to be applied in clinical studies in the nearby future.

6. Challenges and Future Outlook

In spite of the above-discussed advantages of microgel systems in therapeutic and theranostic applications, only few microgel-based systems have been tested in clinical trials.

One of the reasons for this is the potential cellular toxicity of the degradation products of microgels, especially in applications involving intracellular delivery of biomolecular drugs, such as peptides and proteins.[291] Moreover, many stimuli-responsive microgels employ molecular building blocks that are not yet clinically approved. There are only few research groups that investigated long-term stability, degradation profiles, and toxicological effects of individual microgel systems. Clearance from the body is not yet well understood. While renal clearance has been presented for microgels of up to 10 nm,[292] for many microgel systems clearance, attraction of a protein corona and recognition by the immune system are not well understood, especially for long intervals. The understanding of where the particles end up (kidney, liver, spleen, lung, etc.) and their metabolic clearance (renal, hepatic-intestinal, tracheobronchial) is crucial for clinical translation.[153,292] Therefore, for microgel drug delivery systems, there is still a need to clarify the complex degradation and release mechanism.

For the specific treatment of many neurological disorders, the major challenge persists in passing the blood-brain barrier (BBB) without producing toxic substances—microgels have been shown to be able to cross the BBB to deliver oligonucleotides.[293] However, clearance from the brain also needs to be investigated further.

Another major challenge is to deliver sufficient amounts of drug and the independent drug release of dual- and multiple-loaded microgels.[294] Similar to many other nanomedicines, only 5–10% of the injected microgels actually reach the targeted tissue. The tissue distribution and in vivo circulation time is strongly influenced by the size, shape, and charge of the microgels, which also greatly affects their function as imaging vehicles.

In tissue engineering, injectable hydrogel systems are widely investigated and are currently being investigated in clinical trials.[290] There are 425 clinical trials involving natural and synthetic hydrogel materials (ClinicalTrials.gov). Currently, over 30 of these studies are already clinically approved by the FDA (U.S. food and drug administration) and/or EMA (European Medicines Agency).[290] Furthermore, there are 30 ongoing clinical studies of injectable hydrogel systems for tissue regeneration applications.[290] Injectable hydrogels must have a sufficiently low viscosity to be introduced via a needle but contain sufficient elasticity after crosslinking in situ to maintain their injected volume and sustain repetitive load.[290] Microgels can overcome these limitation but the translation of safety and efficacy of therapies tested animal studies to human trials is a major challenge due to many unknowns of the toxicity and fate of the microgels and their degradation products.[295]

Preclinical animal studies can give a first idea of clinical efficacy but due to difference in the physiology and variations in the homology of molecular targets in animals and humans, animal models only offer limited information and transferring this knowledge back to human physiology remains challenging.[295] For example, in the clinical study of lidocaine-loaded microgels for anesthesia application, tail flick latency tests were performed in rats, which may not be comparable to wound pain relief in humans.[296]

Finally, there are technical challenges in the production of microgels, mainly in upscaling of the synthesis of complex geometries and reproducibility in functionalization and loading processes.

Microgel systems have to be designed and developed separately for each clinical application. It has been reported that the entire process starting from the idea, via the stages of clinical trials to clinical application of a hydrogel systems costs between from $ 50 million to up to $ 800 million.[290,297] Similar numbers can be expected for microgel systems, for which

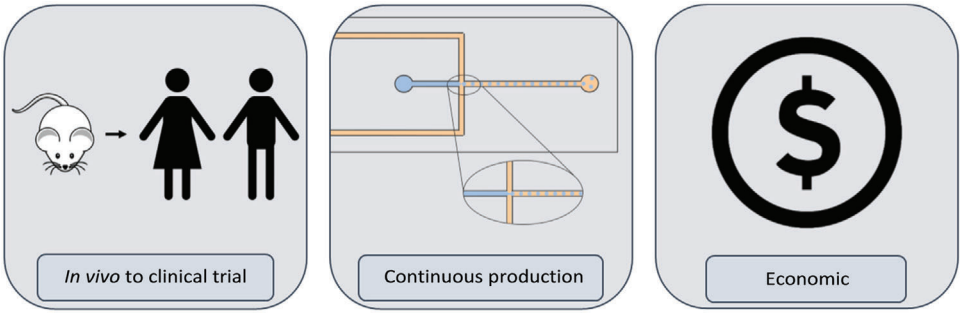

Figure 14. Challenges of microgel application in clinic.

the chemical complexity is comparable to macroscopic hydrogel systems.

In summary, microgel systems represent a versatile platform, and can be loaded by an unprecedented variety of types of cargo, from small molecules to particles and from covalent attachment to physical entrapment in the microgel network. While a variety of challenges remain, therapeutic microgels are powerful entities with superior biomedical properties. They have great potential to become the solution for many unanswered therapeutic and imaging problems of the future.

Acknowledgements

A.J.C.K. and L.D.L. contributed equally to this work. The authors acknowledge funding by the collaborative research center on microgels SFB 985, funded by the Deutsche Forschungsgemeinschaft (DFG).

Open access funding enabled and organized by Projekt DEAL.

Conflict of Interest

The authors declare no conflict of interest.

Keywords

biomedical applications, clinic, microgels, theranostics

Received: September 17, 2021
Revised: November 17, 2021
Published online: December 11, 2021

[1] E. M. Ahmed, *J. Adv. Res.* **2015**, *6*, 105.
[2] E. Caló, V. V. Khutoryanskiy, *Eur. Polym. J.* **2015**, *65*, 252.
[3] O. Erol, A. Pantula, W. Liu, D. H. Gracias, *Adv. Mater. Technol.* **2019**, *4*, 1900043.
[4] J. C. Rose, L. De Laporte, *Adv. Healthcare Mater.* **2018**, *7*, 1701067.
[5] J. J. Rice, M. M. Martino, L. De Laporte, F. Tortelli, P. S. Briquez, J. A. Hubbell, *Adv. Healthcare Mater.* **2013**, *2*, 57.
[6] J. A. Bonham, M. A. Faers, J. S. Van Duijneveldt, *Soft Matter* **2014**, *10*, 9384.
[7] M. E. S. Miranda, C. Marcolla, C. A. Rodrígues, H. M. Wilhelm, M. R. Sierakowski, T. M. B. Bresolin, R. A. Freitas, *Polym. Int.* **2006**, *55*, 961.
[8] F. Sanchez, K. Sobolev, *Constr. Build. Mater.* **2010**, *24*, 2060.
[9] G. Guisbiers, S. Mejía-Rosales, F. L. Deepak, *J. Nanomater.* **2012**, *2012*, 180976.
[10] A. J. D. Krüger, O. Bakirman, L. P. B. Guerzoni, A. Jans, D. B. Gehlen, D. Rommel, T. Haraszti, A. J. C. Kuehne, L. De Laporte, *Adv. Mater.* **2019**, *31*, 1903668.
[11] A. J. D. Krüger, J. Köhler, S. Cichosz, J. C. Rose, D. B. Gehlen, T. Haraszti, M. Möller, L. De Laporte, *Chem. Commun.* **2018**, *54*, 6943.
[12] L. M. T. Martinez, O. V. Kharissova, B. I. Kharisov, in *Handbook of Ecomaterials* (Eds.: M. Ahumada, E. Jacques, C. Calderon, F. Martínez-Gómez), Springer-Verlag, Berlin, Heidelberg **2017**, pp. 1–20.
[13] M. Chan, A. Almutairi, *Mater. Horiz.* **2016**, *3*, 21.
[14] J. Zhu, W. Sun, J. Zhang, Y. Zhou, M. Shen, C. Peng, X. Shi, *Bioconjugate Chem.* **2017**, *28*, 2692.
[15] V. Keskar, N. W. Marion, J. J. Mao, R. A. Gemeinhart, *Tissue Eng., Part A* **2009**, *15*, 1695.
[16] J. Sun, D. Wei, Y. Zhu, M. Zhong, Y. Zuo, H. Fan, X. Zhang, *Biomaterials* **2014**, *35*, 4759.
[17] H. Wang, S. C. Heilshorn, *Adv. Mater.* **2015**, *27*, 3717.
[18] M. J. Webber, P. Y. W. Dankers, *Macromol. Biosci.* **2019**, *19*, 1800452.
[19] M. Diba, S. Spaans, S. I. S. Hendrikse, M. M. C. Bastings, M. J. G. Schotman, J. F. van Sprang, D. J. Wu, F. J. M. Hoeben, H. M. Janssen, P. Y. W. Dankers, *Adv. Mater.* **2021**, *33*, 2008111.
[20] D. Seliktar, *Science* **2012**, *336*, 1124.
[21] A. Vashist, A. K. Kaushik,S. Ahmad, M. Nair, *Nanogels for Biomedical Applications*, Royal Society of Chemistry, Cambridge **2018**.
[22] M. H. Chen, J. J. Chung, J. E. Mealy, S. Zaman, E. C. Li, M. F. Arisi, P. Atluri, J. A. Burdick, *Macromol. Biosci.* **2019**, *19*, 1800248.
[23] D. F. Emerich, C. G. Thanos, *Expert Opin. Biol. Ther.* **2003**, *3*, 655.
[24] E. Mauri, S. M. Giannitelli, M. Trombetta, A. Rainer, *Gels* **2021**, *7*, 36.
[25] Y. Bin Hamzah, S. Hashim, W. A. W. A. Rahman, *J. Polym. Res.* **2017**, *24*, 134.
[26] D. Suzuki, K. Horigome, T. Kureha, S. Matsui, T. Watanabe, *Polym. J.* **2017**, *49*, 695.
[27] M. Karg, A. Pich, T. Hellweg, T. Hoare, L. A. Lyon, J. J. Crassous, D. Suzuki, R. A. Gumerov, S. Schneider, I. I. Potemkin, W. Richtering, *Langmuir* **2019**, *35*, 6231.
[28] N. M. B. Smeets, T. Hoare, *J. Polym. Sci., Part A: Polym. Chem.* **2013**, *51*, 3027.
[29] S. Seiffert, *Angew. Chem., Int. Ed.* **2013**, *52*, 11462.
[30] Y. Hertle, T. Hellweg, *J. Mater. Chem. B* **2013**, *1*, 5874.
[31] C. Echeverria, S. Fernandes, M. Godinho, J. Borges, P. Soares, *Gels* **2018**, *4*, 54.
[32] R. Pelton, *Adv. Colloid Interface Sci.* **2000**, *85*, 1.
[33] P. Saha, R. Ganguly, X. Li, R. Das, N. K. Singha, A. Pich, *Macromol. Rapid Commun.* **2021**, *42*, 2100112.
[34] S. Singh, M. Möller, A. Pich, *J. Polym. Sci., Part A: Polym. Chem.* **2013**, *51*, 3044.

[35] S. Saxena, C. E. Hansen, L. A. Lyon, *Acc. Chem. Res.* **2014**, *47*, 2426.
[36] F. A. Plamper, W. Richtering, *Acc. Chem. Res.* **2017**, *50*, 131.
[37] T. Kamperman, M. Karperien, S. Le Gac, J. Leijten, *Trends Biotechnol.* **2018**, *36*, 850.
[38] W. Jiang, M. Li, Z. Chen, K. W. Leong, *Lab Chip* **2016**, *16*, 4482.
[39] S. Kühn, J. Sievers, A. Stoppa, N. Träber, R. Zimmermann, P. B. Welzel, C. Werner, *Adv. Funct. Mater.* **2020**, *30*, 1908857.
[40] B. Stawicki, T. Schacher, H. Cho, *Gels* **2021**, *7*, 63.
[41] V. Baskar, I. Salim Meeran, A. Subramani, Sruthi, A. Jawahar, T. K. Shabeer, *Int. J. Pharm. Pharm. Sci.* **2018**, *10*, 1.
[42] A. J. Sivaram, P. Rajitha, S. Maya, R. Jayakumar, M. Sabitha, *Wiley Interdiscip. Rev.: Nanomed. Nanobiotechnol.* **2015**, *7*, 509.
[43] S. S. Das, P. Bharadwaj, M. Bilal, M. Barani, A. Rahdar, P. Taboada, S. Bungau, G. Z. Kyzas, *Polymers (Basel)* **2020**, *12*, 1397.
[44] Y. Jiang, J. Chen, C. Deng, E. J. Suuronen, Z. Zhong, *Biomaterials* **2014**, *35*, 4969.
[45] M. A. Grimaudo, A. Concheiro, C. Alvarez-Lorenzo, *J. Controlled Release* **2019**, *313*, 148.
[46] A. C. Daly, L. Riley, T. Segura, J. A. Burdick, *Nat. Rev. Mater.* **2020**, *5*, 20.
[47] M. D. Neto, M. B. Oliveira, J. F. Mano, *Trends Biotechnol.* **2019**, *37*, 1011.
[48] J. M. Anderson, *Polym. Sci.: Compr. Ref.* **2012**, *9*, 363.
[49] S. Naahidi, M. Jafari, M. Logan, Y. Wang, Y. Yuan, H. Bae, B. Dixon, P. Chen, *Biotechnol. Adv.* **2017**, *35*, 530.
[50] K. Xue, X. Wang, P. W. Yong, D. J. Young, Y.-L. Wu, Z. Li, X. J. Loh, *Adv. Ther.* **2019**, *2*, 1800088.
[51] M. D. Swartzlander, C. A. Barnes, A. K. Blakney, J. L. Kaar, T. R. Kyriakides, S. J. Bryant, *Biomaterials* **2015**, *41*, 26.
[52] E. Bakaic, N. M. B. Smeets, T. Hoare, *RSC Adv.* **2015**, *5*, 35469.
[53] P. J. LeValley, R. Neelarapu, B. P. Sutherland, S. Dasgupta, C. J. Kloxin, A. M. Kloxin, *J. Am. Chem. Soc.* **2020**, *142*, 4671.
[54] V. K. Garripelli, J. K. Kim, R. Namgung, W. J. Kim, M. A. Repka, S. Jo, *Acta Biomater.* **2010**, *6*, 477.
[55] J. Hu, Y. Chen, Y. Li, Z. Zhou, Y. Cheng, *Biomaterials* **2017**, *112*, 133.
[56] S. Pradhan, K. A. Keller, J. L. Sperduto, J. H. Slater, *Adv. Healthcare Mater.* **2017**, *6*, 1700681.
[57] F. Alexis, E. Pridgen, L. K. Molnar, O. C. Farokhzad, *Mol. Pharmaceutics* **2008**, *5*, 505.
[58] M. B. Browning, S. N. Cereceres, P. T. Luong, E. M. Cosgriff-Hernandez, *J. Biomed. Mater. Res., Part A* **2014**, *102*, 4244.
[59] M. B. Browning, E. Cosgriff-Hernandez, *Biomacromolecules* **2012**, *13*, 779.
[60] D. Y. Lee, K. Choe, Y. J. Jeong, J. Yoo, S. M. Lee, J. H. Park, P. Kim, Y. C. Kim, *RSC Adv.* **2015**, *5*, 14482.
[61] R. Luxenhofer, M. Bezen, R. Jordan, *Macromol. Rapid Commun.* **2008**, *29*, 1509.
[62] S. M. Grayson, W. T. Godbey, *J. Drug Target.* **2008**, *16*, 329.
[63] C. X. Wang, S. Utech, J. D. Gopez, M. F. J. Mabesoone, C. J. Hawker, D. Klinger, *ACS Appl. Mater. Interfaces* **2016**, *8*, 16914.
[64] Y. Chen, N. Ballard, S. A. F. Bon, *Polym. Chem.* **2013**, *4*, 387.
[65] Y. Azuma, T. Terashima, M. Sawamoto, *Macromolecules* **2017**, *50*, 587.
[66] F. García, M. M. J. Smulders, *J. Polym. Sci., Part A: Polym. Chem.* **2016**, *54*, 3551.
[67] A. C. Brown, S. E. Stabenfeldt, B. Ahn, R. T. Hannan, K S. Dhada, E. S. Herman, V. Stefanelli, N. Guzzetta, A. Alexeev, W. A. Lam, L. A Lyon, T. H. Barker, *Nat. Mater.* **2014**, *13*, 1108.
[68] H. Bachman, A. C. Brown, K. C. Clarke, K. S. Dhada, A. Douglas, C. E. Hansen, E. Herman, J. S. Hyatt, P. Kodlekere, Z. Meng, S. Saxena, M. W. Spears Jr, N. Welsch, L. A Lyon, *Soft Matter* **2015**, *11*, 2018.
[69] J. Liu, Y. Pang, S. Zhang, C. Cleveland, X. Yin, L. Booth, J. Lin, Y-Ah Lucy Lee, H. Mazdiyasni, S. Saxton, A. R. Kirtane, T. V. Erlach, J. Rogner, R. Langer, G. Traverso, *Nat. Commun.* **2017**, *8*, 124.
[70] C. B. Rodell, J. W. MacArthur, S. M. Dorsey, R. J. Wade, L. L. Wang, Y. J. Woo, J. A. Burdick, *Adv. Funct. Mater.* **2015**, *25*, 636.
[71] H. K. S. Yadav, N. Anwar, A. Halabi, G. A. Alsalloum, *J. Pharm. Pharm. Res.* **2017**, *1*, 5.
[72] D. Klinger, K. Landfester, *Polymer (Guildf)* **2012**, *53*, 5209.
[73] J. S. Varghese, N. Chellappa, N. N. Fathima, *Colloids Surf., B* **2014**, *113*, 346.
[74] S. Allazetta, M. P. Lutolf, *Curr. Opin. Biotechnol.* **2015**, *35*, 86.
[75] Q. Feng, D. Li, Q. Li, X. Cao, H. Dong, *Bioact. Mater.* **2021**, *9*, 105.
[76] K. H. Bae, L. S. Wang, M. Kurisawa, *J. Mater. Chem. B* **2013**, *1*, 5371.
[77] S. Boesveld, A. Jans, D. Rommel, M. Bartneck, M. Möller, L. Elling, C. Trautwein, P. Strnad, A. J. C. Kuehne, *ACS Appl. Mater. Interfaces* **2019**, *11*, 25017.
[78] M. Alvarado-Velez, S. B. Pai, R. V. Bellamkonda, *IEEE Trans. Biomed. Eng.* **2014**, *61*, 1474.
[79] A. Singh, N. A. Peppas, *Adv. Mater.* **2014**, *26*, 6530.
[80] J. C. Rose, D. B. Gehlen, T. Haraszti, J. Köhler, C. J. Licht, L. De Laporte, *Biomaterials* **2018**, *163*, 128.
[81] U. S. Food, E. Marb, *Nat. Biomed. Eng.* **2018**, *2*, 339.
[82] V. F. M. Segers, R. T. Lee, *Nature* **2008**, *451*, 937.
[83] L. M. Marquardt, S. C. Heilshorn, *Physiol. Behav.* **2016**, *2*, 207.
[84] L. P. B. Guerzoni, J. C. Rose, D. B. Gehlen, A. Jans, T. Haraszti, M. Wessling, A. J. C. Kuehne, L. De Laporte, *Small* **2019**, *15*, 1900692.
[85] G. Choe, S. W. Kim, J. Park, J. Park, S. Kim, Y. S. Kim, Y. Ahn, D. W. Jung, D. R. Williams, J. Y. Lee, *Biomaterials* **2019**, *225*, 119513.
[86] A. S. Mao, J. W. Shin, S. Utech, H. Wang, O. Uzun, W. Li, M. Cooper, Y. Hu, L. Zhang, D. A. Weitz, D. J. Mooney, *Nat. Mater.* **2017**, *16*, 236.
[87] D. R. Griffin, W. M. Weaver, P. Scumpia, D. Di Carlo, T. Segura, *Nat. Mater.* **2015**, *14*, 737.
[88] S. R. Caliari, J. A. Burdick, *Nat. Methods.* **2016**, *13*, 405.
[89] T. Kamperman, S. Henke, A. van den Berg, S. R. Shin, A. Tamayol, A. Khademhosseini, M. Karperien, J. Leijten, *Adv. Healthcare Mater.* **2017**, *6*, 1600913.
[90] D. Husman, P. B. Welzel, S. Vogler, L. J. Bray, N. Träber, J. Friedrichs, V. Körber, M. V. Tsurkan, U. Freudenberg, J. Thiele, C. Werner, *Biomater. Sci.* **2020**, *8*, 101.
[91] J. Maitra, V. K. Shukla, *Am. J. Polym. Sci.* **2014**, *4*, 25.
[92] J. K. Oh, R. Drumright, D. J. Siegwart, K. Matyjaszewski, *Prog. Polym. Sci.* **2008**, *33*, 448.
[93] D. Crespy, K. Landfester, *Beilstein J. Org. Chem.* **2010**, *6*, 1132.
[94] T. Tadros, in *Encyclopedia of Colloid and Interface Science* (Ed.: T. Tadros), Springer-Verlag, Berlin, Heidelberg **2013**, pp. 685–731.
[95] S. Kawaguchi, K. Ito, *Adv. Polym. Sci.* **2005**, *175*, 299.
[96] V. Chaudhary, S. Sharma, *J. Polym. Res.* **2019**, *26*, 102.
[97] A. Pich, W. Richtering, *Chemical Design of Responsive Microgels*, Vol. *234*, Springer-Verlag, Berlin, Heidelberg **2010**.
[98] R. Tiwari, T. Heuser, E. Weyandt, B. Wang, A. Walther, *Soft Matter* **2015**, *11*, 8342.
[99] K. Han, R. Tiwari, T. Heuser, A. Walther, *Macromol. Rapid Commun.* **2016**, *37*, 1323.
[100] K. T. M. Tran, T. D. Nguyen, *J. Sci.: Adv. Mater. Devices* **2017**, *2*, 1.
[101] H. Zhang, J. K. Nunes, S. E. A. Gratton, K. P. Herlihy, P. D. Pohlhaus, J. M. DeSimone, *New J. Phys.* **2009**, *11*, 075018.
[102] J. C. Rose, M. Cámara-Torres, K. Rahimi, J. Köhler, M. Möller, L. De Laporte, *Nano Lett.* **2017**, *17*, 3782.
[103] D. Liu, H. Zhang, F. Fontana, J. T. Hirvonen, H. A. Santos, *Adv. Drug Delivery Rev.* **2018**, *128*, 54.
[104] T. Heida, O. Otto, D. Biedenweg, N. Hauck, J. Thiele, *Polymers (Basel)* **2020**, *12*, 1760.
[105] L. P. B. Guerzoni, J. Bohl, A. Jans, J. C. Rose, J. Koehler, A. J. C. Kuehne, L. De Laporte, *Biomater. Sci.* **2017**, *5*, 1549.
[106] D. Hovermann, T. Rossow, R. J. Gübeli, S. Seiffert, W. Weber, *Macromol. Biosci.* **2014**, *14*, 1730.

[107] D. Steinhilber, T. Rossow, S. Wedepohl, F. Paulus, S. Seiffert, R. Haag, *Angew. Chem., Int. Ed.* **2013**, *52*, 13538.
[108] E. Stengelin, A. Kuzmina, G. L. Beltramo, M. F. Koziol, L. Besch, R. Schröder, R. E. Unger, W. Tremel, S. Seiffert, *Adv. Healthcare Mater.* **2020**, *9*, 1901820.
[109] T. Rossow, J. A. Heyman, A. J. Ehrlicher, A. Langhoff, D. A. Weitz, R. Haag, S. Seiffert, *J. Am. Chem. Soc.* **2012**, *134*, 4983.
[110] K. W. Bong, J. Lee, P. S. Doyle, *Lab Chip* **2014**, *14*, 4680.
[111] H. J. M. Wolff, J. Linkhorst, T. Göttlich, J. Savinsky, A. J. D. Krüger, L. De Laporte, M. Wessling, *Lab Chip* **2020**, *20*, 285.
[112] J. R. Tumbleston, D. Shirvanyants, N. Ermoshkin, R. Janusziewicz, A. R. Johnson, D. Kelly, K. Chen, R. Pinschmidt, J. P. Rolland, A. Ermoshkin, E. D. Samulski, J. M. Desimone, *Science (80-.)* **2015**, *347*, 1349.
[113] D. Dendukuri, S. S. Gu, D. C. Pregibon, T. A. Hatton, P. S. Doyle, *Lab Chip* **2007**, *7*, 818.
[114] N. Sanson, J. Rieger, *Polym. Chem.* **2010**, *1*, 965.
[115] M. Suhail, J. M. Rosenholm, M. U. Minhas, S. F. Badshah, A. Naeem, K. U. Khan, M. Fahad, *Ther. Delivery* **2019**, *10*, 697.
[116] P. Boisseau, B. Loubaton, *C. R. Phys.* **2011**, *12*, 620.
[117] S. Sinjari, J. S. Freitag, C. Herold, O. Otto, D. M. Smith, H. D. H. Stöver, *J. Polym. Sci.* **2020**, *58*, 2317.
[118] S. Girardo, N. Träber, K. Wagner, G. Cojoc, C. Herold, R. Goswami, R. Schlüßler, S. Abuhattum, A. Taubenberger, F. Reichel, D. Mokbel, M. Herbig, M. Schürmann, P. Müller, T. Heida, A. Jacobi, E. Ulbricht, J. Thiele, C. Werner, J. Guck, *J. Mater. Chem. B* **2018**, *6*, 6245.
[119] R. Schlüßler, K. Kim, M. Nötzel, A. Taubenberger, S. Abuhattum, T. Beck, P. Müller, S. Maharana, G. Cojoc, A. Hermann, S. Alberti, J. Guck, *bioRxiv* **2020**, 2020.10.30.361808.
[120] N. Hauck, N. Seixas, S. P. Centeno, R. Schlüßler, G. Cojoc, P. Müller, J. Guck, D. Wöll, L. A. Wessjohann, J. Thiele, *Polymers (Basel)* **2018**, *10*, 1055.
[121] T. G. F. Souza, V. S. T. Ciminelli, N. D. S. Mohallem, *J. Phys.: Conf. Ser.* **2016**, *733*, 012039.
[122] T. Kureha, H. Minato, D. Suzuki, K. Urayama, M. Shibayama, *Soft Matter* **2019**, *15*, 5390.
[123] R. K. Nicholas Dias, Y. Peng, *Anal. Biochem.* **2016**, *501*, 4.
[124] K. Horigome, T. Ueki, D. Suzuki, *Polym. J.* **2016**, *48*, 273.
[125] M. Koch, M. K. Włodarczyk-Biegun, *Bioprinting* **2020**, *20*, e00098.
[126] R. Cui, Z. Zhang, J. Nie, B. Du, *Colloid Polym. Sci.* **2017**, *295*, 665.
[127] B. Krug, N. Koukourakis, J. W. Czarske, *Opt. Express* **2019**, *27*, 26910.
[128] R. Macháň, Y. H. Foo, T. Wohland, *Biophys. J.* **2016**, *111*, 152.
[129] D. Wöll, *RSC Adv.* **2014**, *4*, 2447.
[130] B. L. Sprague, J. G. McNally, *Trends Cell Biol.* **2005**, *15*, 84.
[131] A. Balaceanu, D. E. Demco, M. Möller, A. Pich, *Macromolecules* **2011**, *212*, 2161.
[132] A. Balaceanu, D. E. Demco, M. Möller, A. Pich, *Macromol. Chem. Phys.* **2011**, *212*, 2467.
[133] G. Aguirre, A. Khoukh, K. Chougrani, V. Alard, L. Billon, *Polym. Chem.* **2018**, *9*, 757.
[134] B. Sierra-Martín, M. S. Romero-Cano, T. Cosgrove, B. Vincent, A. Fernández-Barbero, *Colloids Surf., A* **2005**, *270–271*, 296.
[135] M. Kappl, H. J. Butt, *Part. Part. Syst. Charact.* **2002**, *19*, 129.
[136] A. Mark, N. Helfricht, A. Rauh, M. Karg, G. Papastavrou, *Small* **2019**, *15*, 1902976.
[137] A. Aufderhorst-Roberts, D. Baker, R. J. Foster, O. Cayre, J. Mattsson, S. D. Connell, *Nanoscale* **2018**, *10*, 16050.
[138] S. Bhattacharjee, *J. Controlled Release* **2016**, *235*, 337.
[139] A. D. Levin, E. A. Shmytkova, B. N. Khlebtsov, *J. Phys. Chem. C* **2017**, *121*, 3070.
[140] E. Siemes, O. Nevskyi, D. Sysoiev, S. K. Turnhoff, A. Oppermann, T. Huhn, W. Richtering, D. Wöll, *Angew. Chem., Int. Ed.* **2018**, *57*, 12280.
[141] L. L. E. Mears, E. R. Draper, A. M. Castilla, H. Su, Zhuola, B. Dietrich, M. C. Nolan, G. N. Smith, J. Doutch, S. Rogers, R. Akhtar, H. Cui, D. J. Adams, *Biomacromolecules* **2017**, *18*, 3531.
[142] M. Serna, *Front. Mol. Biosci.* **2019**, *6*, 33.
[143] T. Nakane, A. Kotecha, A. Sente, G. McMullan, S. Masiulis, P. M. G. E. Brown, I. T. Grigoras, L. Malinauskaite, T. Malinauskas, J. Miehling, T. Uchański, L. Yu, D. Karia, E. V. Pechnikova, E. de Jong, J. Keizer, M. Bischoff, J. McCormack, P. Tiemeijer, S. W. Hardwick, D. Y. Chirgadze, G. Murshudov, A. R. Aricescu, S. H. W. Scheres, *Nature* **2020**, *587*, 152.
[144] D. K. Baby, in *Rheology of Polymer Blends and Nanocomposites* (Eds.: S. Thomas, C. Sarathchandran, N. Chandran), Elsevier Inc., **2019**, pp. 193–204.
[145] P. E. Bunney, A. N. Zink, A. A. Holm, C. J. Billington, C. M. Kotz, *Physiol. Behav.* **2017**, *176*, 139.
[146] S. Wang, X. Wang, F. G. Draenert, O. Albert, H. C. Schröder, V. Mailänder, G. Mitov, W. E. G. Müller, *Bone* **2014**, *67*, 292.
[147] N. Jalili, K. Laxminarayana, *Mechatronics* **2004**, *14*, 907.
[148] C. Yu, J. Liu, G. Lu, Y. Xie, Y. Sun, Q. Wang, J. Liang, Y. Fan, X. Zhang, *J. Mater. Chem. B* **2018**, *6*, 5164.
[149] M. M. Villone, J. K. Nunes, Y. Li, H. A. Stone, P. L. Maffettone, *Soft Matter* **2019**, *15*, 880.
[150] L. Nyström, R. Nordström, J. Bramhill, B. R. Saunders, R. Álvarez-Asencio, M. W. Rutland, M. Malmsten, *Biomacromolecules* **2016**, *17*, 669.
[151] J. Friedrichs, J. M. Torkko, J. Helenius, T. P. Teräväinen, J. Füllekrug, D. J. Muller, K. Simons, A. Manninen, *J. Biol. Chem.* **2007**, *282*, 29375.
[152] M. Mokbel, D. Mokbel, A. Mietke, N. Träber, S. Girardo, O. Otto, J. Guck, S. Aland, *ACS Biomater. Sci. Eng.* **2017**, *3*, 2962.
[153] K. S. Soni, S. S. Desale, T. K. Bronich, *J Control. Release* **2016**, *240*, 109.
[154] G. Agrawal, R. Agrawal, *Small* **2018**, *14*, 1801724.
[155] I. Neamtu, A. G. Rusu, A. Diaconu, L. E. Nita, A. P. Chiriac, *Drug Delivery* **2017**, *24*, 539.
[156] H. Cho, U. Jammalamadaka, K. Tappa, *Materials (Basel)* **2018**, *11*, 302.
[157] F. Sultana, Manirujjaman, M. Imran-Ul-Haque, M. Arafat, S. Sharmin, *J. Appl. Pharm. Sci.* **2013**, *3*, 95.
[158] N. S. Zarekar, V. J. Lingayat, V. V Pande, *Nanosci. Nanotechnol. Res.* **2017**, *4*, 25.
[159] X. Huang, C. S. Brazel, *J. Controlled Release* **2001**, *73*, 121.
[160] J. Yoo, Y. Y. Won, *ACS Biomater. Sci. Eng.* **2020**, *6*, 6053.
[161] A. J. Thote, J. T. Chappell, R. B. Gupta, R. Kumar, *Drug Dev. Ind. Pharm.* **2005**, *31*, 43.
[162] M. C. García, J. C. Cuggino, in *Stimulus-responsive Polymeric Nanocarriers for Drug Delivery Applications – Types and Triggers* (Eds.: A. S. H. Makhlouf, N. Y. Abu-Thabit), vol. *1*, Elsevier, Amsterdam **2018**, pp. 321–338.
[163] L. Zha, B. Banik, F. Alexis, *Soft Matter* **2011**, *7*, 5908.
[164] T. Yoshida, T. C. Lai, G. S. Kwon, K. Sako, *Expert Opin. Drug Delivery* **2013**, *10*, 1497.
[165] Z. Li, J. Huang, J. Wu, *Biomater. Sci.* **2021**, *9*, 574.
[166] J. Karnoosh-Yamchi, M. Mobasseri, A. Akbarzadeh, S. Davaran, A. R. Ostad-Rahimi, H. Hamishehkar, R. Salehi, Z. Bahmani, K. Nejati-Koshki, A. Darbin, M. Rahmati-Yamchi, *Mol. Biol. Rep.* **2014**, *41*, 6705.
[167] W. Gao, J. Chan, O. C. Farokhzad, *Bone* **2010**, *7*, 1913.
[168] G. Yang, X. Wang, S. Fu, R. Tang, J. Wang, *Acta Biomater.* **2017**, *60*, 232.
[169] Y. Zhao, C. Simon, M. Daoud Attieh, K. Haupt, A. Falcimaigne-Cordin, *RSC Adv.* **2020**, *10*, 5978.
[170] M. P. Gamcsik, M. S. Kasibhatla, S. D. Teeter, O. M. Colvin, *Biomarkers* **2012**, *17*, 671.

[171] X. Liu, J. Wang, W. Xu, J. Ding, B. Shi, K. Huang, X. Zhuang, X. Chen, *Int. J. Nanomed.* **2015**, *10*, 6587.
[172] N. Drude, O. H. Winz, F. M. Mottaghy, M. Roller, H. Königs, M. Möller, S. Singh, A. Morgenroth, *Small* **2018**, *14*, 1704093.
[173] L. Massi, A. Najer, R. Chapman, C. D. Spicer, V. Nele, J. Che, M. A. Booth, J. J. Doutch, M. M. Stevens, *J. Mater. Chem. B* **2020**, *8*, 8894.
[174] Y. Wang, Y. Luo, Q. Zhao, Z. Wang, Z. Xu, X. Jia, *ACS Appl. Mater. Interfaces* **2016**, *8*, 19899.
[175] C. Yang, X. Wang, X. Yao, Y. Zhang, W. Wu, X. Jiang, *J. Controlled Release* **2015**, *205*, 206.
[176] Q. Guo, X. Zhang, *J. Biomater. Sci., Polym. Ed.* **2019**, *30*, 815.
[177] M. Vicario-de-la-Torre, J. Forcada, *Gels* **2017**, *3*, 16.
[178] X. Wang, D. Niu, P. Li, Q. Wu, X. Bo, B. Liu, S. Bao, T. Su, H. Xu, Q. Wang, *ACS Nano* **2015**, *9*, 5646.
[179] D. C. Leite, S. Kakorin, Y. Hertle, T. Hellweg, N. P. da Silveira, *Langmuir* **2018**, *34*, 10943.
[180] Z. Zhang, H. Li, S. Kasmi, S. Van Herck, K. Deswarte, B. N. Lambrecht, R. Hoogenboom, L. Nuhn, B. G. De Geest, *Angew. Chem., Int. Ed.* **2019**, *58*, 7866.
[181] M. Ohshio, K. Ishihara, A. Maruyama, N. Shimada, S. I. Yusa, *Langmuir* **2019**, *35*, 7261.
[182] Y. Kotsuchibashi, *Polym. J.* **2020**, *52*, 681.
[183] N. Shimada, T. Sasaki, T. Kawano, A. Maruyama, *Biomacromolecules* **2018**, *19*, 4133.
[184] A. Fujihara, K. Itsuki, N. Shimada, A. Maruyama, N. Sagawa, T. Shikata, S. I. Yusa, *J. Polym. Sci., Part A: Polym. Chem.* **2016**, *54*, 2845.
[185] R. Rajan, K. Matsumura, *Macromol. Rapid Commun.* **2017**, *38*, 1700478.
[186] R. Rajan, K. Matsumura, *J. Mater. Chem. B* **2015**, *3*, 5683.
[187] M. Seuss, W. Schmolke, A. Drechsler, A. Fery, S. Seiffert, *ACS Appl. Mater. Interfaces* **2016**, *8*, 16317.
[188] C. G. Lopez, T. Lohmeier, J. E. Wong, W. Richtering, *J. Colloid Interface Sci.* **2019**, *558*, 200.
[189] C. Hu, W. Xu, C. M. Conrads, J. Wu, A. Pich, *J. Colloid Interface Sci.* **2021**, *582*, 1075.
[190] C. Echeverria, C. Mijangos, *Langmuir* **2011**, *27*, 8027.
[191] A. M. Schmidt, *Colloid Polym. Sci.* **2007**, *285*, 953.
[192] S. Chen, Q. Bian, P. Wang, X. Zheng, L. Lv, Z. Dang, G. Wang, *Polym. Chem.* **2017**, *8*, 6150.
[193] D. Gyawali, J. P. Kim, J. Yang, *Bioact. Mater.* **2018**, *3*, 39.
[194] J. Yang, Y. Zhang, S. Gautam, L. Liu, J. Dey, W. Chen, R. P. Mason, C. A. Serrano, K. A. Schug, L. Tang, *Proc. Natl. Acad. Sci. U. S. A.* **2009**, *106*, 10086.
[195] E. Mueller, S. Himbert, M. J. Simpson, M. Bleuel, M. C. Rheinstadter, T. Hoare, *Macromolecules* **2021**, *54*, 351.
[196] A. Chanmugam, D. Langemo, K. Thomason, J. Haan, E. A. Altenburger, A. Tippett, L. Henderson, T. A. Zortman, *Adv. Skin Wound Care* **2017**, *30*, 406.
[197] J. Yeo, Y. M. Lee, J. Lee, D. Park, K. Kim, J. Kim, J. Park, W. J. Kim, *Nano Lett.* **2019**, *19*, 6716.
[198] J. Yeo, J. Lee, S. Yoon, W. J. Kim, *Biomater. Sci.* **2020**, *8*, 1148.
[199] S. Kumar, S. Sharma, N. Vasudeva, *Chin. J. Integr. Med.* **2017**, https://doi.org/10.1007/s11655-017-2414-z.
[200] A. Jans, R. R. Rosencrantz, A. D. Mandić, N. Anwar, S. Boesveld, C. Trautwein, M. Moeller, G. Sellge, L. Elling, A. J. C. Kuehne, *Biomacromolecules* **2017**, *18*, 1460.
[201] S. Das, P. Angsantikul, C. Le, D. Bao, Y. Miyamoto, W. Gao, L. Zhang, L. Eckmann, *PLoS Neglected Trop. Dis.* **2018**, *12*, e0006266.
[202] D. D. Zomer-Van Ommen, A. V. Pukin, O. Fu, L. H. C. Quarles Van Ufford, H. M. Janssens, J. M. Beekman, R. J. Pieters, *J. Med. Chem.* **2016**, *59*, 6968.
[203] T. J. Paul, S. Rübel, M. Hildebrandt, A. K. Strzelczyk, C. Spormann, T. K. Lindhorst, S. Schmidt, *ACS Appl. Mater. Interfaces* **2019**, *11*, 26674.
[204] M. Zan, J. Li, M. Huang, S. Lin, D. Luo, S. Luo, Z. Ge, *Biomater. Sci.* **2015**, *3*, 1147.
[205] V. Alakhov, G. Pietrzynski, K. Patel, A. Kabanov, L. Bromberg, T. A. Hatton, *J. Pharm. Pharmacol.* **2004**, *56*, 1233.
[206] H. Qiao, X. Chen, Q. Wang, J. Zhang, D. Huang, E. Chen, H. Qian, Y. Zhong, Q. Tang, W. Chen, *Biomater. Sci.* **2020**, *8*, 2472.
[207] M. Look, E. Stern, Q. A. Wang, L. D. DiPlacido, M. Kashgarian, J. Craft, T. M. Fahmy, *J. Clin. Invest.* **2013**, *123*, 1741.
[208] C. Y. Gong, Q. J. Wu, Y. J. Wang, D. D. Zhang, F. Luo, X. Zhao, Y. Q. Wei, Z. Y. Qian, *Biomaterials* **2013**, *34*, 6377.
[209] H. Ayame, N. Morimoto, K. Akiyoshi, *Bioconjugate Chem.* **2008**, *19*, 882.
[210] T. Nochi, Y. Yuki, H. Takahashi, S. I. Sawada, M. Mejima, T. Kohda, N. Harada, I. G. Kong, A. Sato, N. Kataoka, D. Tokuhara, S. Kurokawa, Y. Takahashi, H. Tsukada, S. Kozaki, K. Akiyoshi, H. Kiyono, *Nat. Mater.* **2010**, *9*, 572.
[211] G. Divya, R. Panonnummal, S. Gupta, R. Jayakumar, M. Sabitha, *Eur. J. Pharm. Biopharm.* **2016**, *107*, 97.
[212] M. Van Elk, C. Lorenzato, B. Ozbakir, C. Oerlemans, G. Storm, F. Nijsen, R. Deckers, T. Vermonden, W. E. Hennink, *Eur. Polym. J.* **2015**, *72*, 620.
[213] F. Zabihi, S. Wieczorek, M. Dimde, S. Hedtrich, H. G. Börner, R. Haag, *J. Controlled Release* **2016**, *242*, 35.
[214] S. Okonogi, A. Kaewpinta, S. Yotsawimonwat, S. Khongkhunthian, *Drug Discovery Ther.* **2015**, *9*, 397.
[215] S. Khongkhunthian, T. Sastraruji, S. Klayraung, S. Okonogi, *Drug Discovery Ther.* **2018**, *12*, 31.
[216] S. Kitano, S. Kageyama, Y. Nagata, Y. Miyahara, A. Hiasa, H. Naota, S. Okumura, H. Imai, T. Shiraishi, M. Masuya, M. Nishikawa, J. Sunamoto, K. Akiyoshi, T. Kanematsu, A. M. Scott, R. Murphy, E. W. Hoffman, L. J. Old, H. Shiku, *Clin. Cancer Res.* **2006**, *12*, 7397.
[217] S. Kageyama, S. Kitano, M. Hirayama, Y. Nagata, H. Imai, T. Shiraishi, K. Akiyoshi, A. M. Scott, R. Murphy, E. W. Hoffman, L. J. Old, N. Katayama, H. Shiku, *Cancer Sci.* **2008**, *29*, 601.
[218] B. S. Chandrashekha, M. Anitha, M. Ruparelia, P. Vaidya, R. Aamir, S. Shah, S. Thilak, S. Aurangabadkar, S. Pal, A. Saraswat, J. J. Sanmukhani, *J. Clin. Diagn. Res.* **2015**, *9*, WC04.
[219] B. V. Muniz, D. Baratelli, S. Di Carla, L. Serpe, C. B. Da Silva, V. A. Guilherme, L. N. De M Ribeiro, C. M. S. Cereda, E. De Paula, M. C. Volpato, F. C. Groppo, L. F. Fraceto, M. Franz-Montan, *Sci. Rep.* **2018**, *8*, 17972.
[220] G. Tiwari, R. Tiwari, S. Bannerjee, L. Bhati, S. Pandey, P. Pandey, B. Sriwastawa, *Int. J. Pharm. Invest.* **2012**, *2*, 2.
[221] Y. Nomura, M. Ikeda, N. Yamaguchi, Y. Aoyama, K. Akiyoshi, *FEBS Lett.* **2003**, *553*, 271.
[222] T. Nishikawa, K. Akiyoshi, J. Sunamoto, *J. Am. Chem. Soc.* **1996**, *118*, 6110.
[223] G. F. Webster, *J. Am. Acad. Dermatol.* **1998**, *39*, 38.
[224] H. Wang, Q. Chen, S. Zhou, *Chem. Soc. Rev.* **2018**, *47*, 4198.
[225] M. Tsintou, C. Wang, K. Dalamagkas, D. Weng, Y. N. Zhang, W. Niu, in *Nanobiomaterials Science, Development and Evaluation* (Eds.: M. Razavi, A. Thakor), Elsevier, Amsterdam **2017**, pp. 87–124.
[226] W. Zhou, G. Yang, X. Ni, S. Diao, C. Xie, Q. Fan, *Polymers (Basel)* **2020**, *12*, 1902.
[227] A. Soleimani, F. Martínez, V. Economopoulos, P. J. Foster, T. J. Scholl, E. R. Gillies, *J. Mater. Chem. B* **2013**, *1*, 1027.
[228] M. Chan, J. Lux, T. Nishimura, K. Akiyoshi, A. Almutairi, *Biomacromolecules* **2015**, *16*, 2964.

[229] C. Zhang, W. Sun, Y. Wang, F. Xu, J. Qu, J. Xia, M. Shen, X. Shi, *ACS Appl. Mater. Interfaces* **2020**, *12*, 9107.
[230] Z. Chu, Z. Wang, L. Chen, X. Wang, C. Huang, M. Cui, D. P. Yang, N. Jia, *ACS Appl. Nano Mater.* **2018**, *1*, 2332.
[231] L. Jiang, Q. Zhou, K. Mu, H. Xie, Y. Zhu, W. Zhu, Y. Zhao, H. Xu, X. Yang, *Biomaterials* **2013**, *34*, 7418.
[232] L. E. McInnes, S. E. Rudd, P. S. Donnelly, *Coord. Chem. Rev.* **2017**, *352*, 499.
[233] T. Etrych, H. Lucas, O. Janoušková, P. Chytil, T. Mueller, K. Mäder, *J. Controlled Release* **2016**, *226*, 168.
[234] H. Mok, H. Jeong, S. J. Kim, B. H. Chung, *Chem. Commun.* **2012**, *48*, 8628.
[235] J. Yang, M. H. Yao, D. H. Zhao, X. S. Zhang, R. M. Jin, Y. Di Zhao, B. Liu, *J. Nanopart. Res.* **2017**, *19*, 284.
[236] W. Wu, M. Aiello, T. Zhou, A. Berliner, P. Banerjee, S. Zhou, *Biomaterials* **2010**, *31*, 3023.
[237] M. Liras, I. Quijada-Garrido, O. García, *Polym. Chem.* **2017**, *8*, 5317.
[238] H. Wang, S. Mukherjee, J. Yi, P. Banerjee, Q. Chen, S. Zhou, *ACS Appl. Mater. Interfaces* **2017**, *9*, 18639.
[239] Y. W. Noh, S. H. Kong, D. Y. Choi, H. S. Park, H. K. Yang, H. J. Lee, H. C. Kim, K. W. Kang, M. H. Sung, Y. T. Lim, *ACS Nano* **2012**, *6*, 7820.
[240] T. Jing, L. Fu, L. Liu, L. Yan, *Polym. Chem.* **2016**, *7*, 951.
[241] J. Xia, J. Yao, L. V. Wang, *Prog. Electromagn. Res.* **2014**, *147*, 1.
[242] Y. Zhou, Y. Hu, W. Sun, B. Zhou, J. Zhu, C. Peng, M. Shen, X. Shi, *Nanoscale* **2017**, *9*, 12746.
[243] R. García-Álvarez, L. Chen, A. Nedilko, A. Sánchez-Iglesias, A. Rix, W. Lederle, V. Pathak, T. Lammers, G. Von Plessen, K. Kostarelos, L. M. Liz-Marzán, A. J. C. Kuehne, D. N. Chigrin, *ACS Photonics* **2020**, *7*, 646.
[244] Y. Chandorkar, A. Castro Nava, S. Schweizerhof, M. Van Dongen, T. Haraszti, J. Köhler, H. Zhang, R. Windoffer, A. Mourran, M. Möller, L. De Laporte, *Nat. Commun.* **2019**, *10*, 4027.
[245] M. Das, N. Sanson, D. Fava, E. Kumacheva, *Langmuir* **2007**, *23*, 196.
[246] L. Nie, X. Chen, *Chem. Soc. Rev.* **2014**, *43*, 7132.
[247] N. Singh, L. A. Lyon, *Chem. Mater.* **2007**, *19*, 719.
[248] R. M. Jin, M. H. Yao, J. Yang, D. H. Zhao, Y. Di Zhao, B. Liu, *ACS Sustainable Chem. Eng.* **2017**, *5*, 9841.
[249] W. Sun, J. Zhang, C. Zhang, P. Wang, C. Peng, M. Shen, X. Shi, *ACS Macro Lett.* **2018**, *7*, 137.
[250] Y. Zou, D. Li, Y. Wang, Z. Ouyang, Y. Peng, H. Tomás, J. Xia, J. Rodrigues, M. Shen, X. Shi, *Bioconjugate Chem.* **2020**, *31*, 907.
[251] Y. Zhu, X. Wang, J. Chen, J. Zhang, F. Meng, C. Deng, R. Cheng, J. Feijen, Z. Zhong, *J. Controlled Release* **2016**, *244*, 229.
[252] W. Sun, J. Zhang, C. Zhang, Y. Zhou, J. Zhu, C. Peng, M. Shen, X. Shi, *J. Mater. Chem. B* **2018**, *6*, 4835.
[253] M. R. Gordon, J. Zhuang, J. Ventura, L. Li, K. Raghupathi, S. Thayumanavan, *Mol. Pharmaceutics* **2018**, *15*, 1180.
[254] M. Norouzi, V. Yathindranath, J. A. Thliveris, B. M. Kopec, T. J. Siahaan, D. W. Miller, *Sci. Rep.* **2020**, *10*, 11292.
[255] K. T. Nguyen, J. L. West, *Biomaterials* **2002**, *23*, 4307.
[256] A. Sivashanmugam, R. Arun Kumar, M. Vishnu Priya, S. V. Nair, R. Jayakumar, *Eur. Polym. J.* **2015**, *72*, 543.
[257] A. Al-Abboodi, J. Fu, P. M. Doran, T. T. Y. Tan, P. P. Y. Chan, *Adv. Healthcare Mater.* **2014**, *3*, 725.
[258] J. Kim, M. J. Yaszemski, L. Lu, *Tissue Eng., Part C* **2009**, *15*, 583.
[259] N. Huebsch, E. Lippens, K. Lee, M. Mehta, S. T. Koshy, M. C. Darnell, R. M. Desai, C. M. Madl, M. Xu, X. Zhao, O. Chaudhuri, C. Verbeke, W. S. Kim, K. Alim, A. Mammoto, D. E. Ingber, G. N. Duda, D. J. Mooney, *Nat. Mater.* **2015**, *14*, 1269.
[260] A. Marrella, A. Lagazzo, E. Dellacasa, C. Pasquini, E. Finocchio, F. Barberis, L. Pastorino, P. Giannoni, S. Scaglione, *Polymers (Basel)* **2018**, *10*, 380.
[261] E. Sideris, D. R. Griffin, Y. Ding, S. Li, W. M. Weaver, D. Di Carlo, T. Hsiai, T. Segura, *ACS Biomater. Sci. Eng.* **2016**, *2*, 2034.
[262] J. M. de Rutte, J. Koh, D. Di Carlo, *Adv. Funct. Mater.* **2019**, *29*, 1900071.
[263] L. Pruett, R. Ellis, M. McDermott, C. Roosa, D. Griffin, *J. Mater. Chem. B* **2021**, *9*, 7132.
[264] N. F. Truong, E. Kurt, N. Tahmizyan, S. C. Lesher-Pérez, M. Chen, N. J. Darling, W. Xi, T. Segura, *Acta Biomater.* **2019**, *94*, 160.
[265] J. Fang, J. Koh, Q. Fang, H. Qiu, M. M. Archang, M. M. Hasani-Sadrabadi, H. Miwa, X. Zhong, R. Sievers, D. W. Gao, R. Lee, D. D. Carlo, S. Li, *Adv. Funct. Mater.* **2020**, *30*, 2004307.
[266] L. J. Pruett, C. H. Jenkins, N. S. Singh, K. J. Catallo, D. R. Griffin, *Adv. Funct. Mater.* **2021**, *31*, 2104337.
[267] J. Koh, D. R. Griffin, M. M. Archang, A. C. Feng, T. Horn, M. Margolis, D. Zalazar, T. Segura, P. O. Scumpia, D. Di Carlo, *Small* **2019**, *15*, 1903147.
[268] R. S. Hsu, P. Y. Chen, J. H. Fang, Y. Y. Chen, C. W. Chang, Y. J. Lu, S. H. Hu, *Adv. Sci.* **2019**, *6*, 1900520.
[269] A. J. Seymour, S. Shin, S. C. Heilshorn, *Adv. Healthcare Mater.* **2021**, *10*, 2100644.
[270] N. J. Darling, W. Xi, E. Sideris, A. R. Anderson, C. Pong, S. T. Carmichael, T. Segura, *Adv. Healthcare Mater.* **2020**, *9*, 1901391.
[271] B. N. Pfaff, L. J. Pruett, N. J. Cornell, J. De Rutte, D. Di Carlo, B. Christopher, *ACS Biomater. Sci. Eng.* **2021**, *7*, 422.
[272] D. R. Griffin, M. M. Archang, C. H. Kuan, W. M. Weaver, J. S. Weinstein, A. C. Feng, A. Ruccia, E. Sideris, V. Ragkousis, J. Koh, M. V. Plikus, D. D. Carlo, T. Segura, P. O. Scumpia, *Nat. Mater.* **2021**, *20*, 560.
[273] N. F. Truong, S. C. Lesher-Pérez, E. Kurt, T. Segura, *Bioconjugate Chem.* **2019**, *30*, 476.
[274] C. M. Dumont, M. A. Carlson, M. K. Munsell, A. J. Ciciriello, K. Strnadova, J. Park, B. J. Cummings, A. J. Anderson, L. D. Shea, *Acta Biomater.* **2019**, *86*, 312.
[275] Z. Hu, C. Ma, X. Rong, S. Zou, X. Liu, *ACS Appl. Mater. Interfaces* **2018**, *10*, 2377.
[276] A. S. Caldwell, V. V. Rao, A. C. Golden, D. J. Bell, J. C. Grim, K. S. Anseth, *Bioeng. Transl. Med.* **2021**, *6*, e10217.
[277] J. C. Rose, M. Fölster, L. Kivilip, J. L. Gerardo-Nava, E. E. Jaekel, D. B. Gehlen, W. Rohlfs, L. De Laporte, *Polym. Chem.* **2020**, *11*, 496.
[278] J. C. Rose, D. B. Gehlen, A. Omidinia-Anarkoli, M. Fölster, T. Haraszti, E. E. Jaekel, L. De Laporte, *Adv. Healthcare Mater.* **2020**, *9*, 2000886.
[279] C. Licht, J. C. Rose, A. O. Anarkoli, D. Blondel, M. Roccio, T. Haraszti, D. B. Gehlen, J. A. Hubbell, M. P. Lutolf, L. De Laporte, *Biomacromolecules* **2019**, *20*, 4075.
[280] M. M. Martino, J. A. Hubbell, *FASEB J.* **2010**, *24*, 4711.
[281] L. P. B. Guerzoni, Y. Tsukamoto, D. B. Gehlen, D. Rommel, T. Haraszti, M. Akashi, L. De Laporte, *Biomacromolecules* **2019**, *20*, 3746.
[282] T. Bliss, R. Guzman, M. Daadi, G. K. Steinberg, *Stroke* **2007**, *38*, 817.
[283] P. Assinck, G. J. Duncan, B. J. Hilton, J. R. Plemel, W. Tetzlaff, *Nat. Neurosci.* **2017**, *20*, 637.
[284] S. Rafii, D. Lyden, *Nat. Med.* **2003**, *9*, 702.
[285] P. H. Kim, H. G. Yim, Y. J. Choi, B. J. Kang, J. Kim, S. M. Kwon, B. S. Kim, N. S. Hwang, J. Y. Cho, *J. Controlled Release* **2014**, *187*, 1.
[286] J. Tang, X. Cui, T. G. Caranasos, M. T. Hensley, A. C. Vandergriff, Y. Hartanto, D. Shen, H. Zhang, J. Zhang, K. Cheng, *ACS Nano* **2017**, *11*, 9738.
[287] R. N. Chen, L. W. Lee, L. C. Chen, H. O. Ho, S. C. Lui, M. T. Sheu, C. H. Su, *Int. J. Nanomed.* **2012**, *7*, 4697.
[288] D. Thomas, G. Fontana, X. Chen, C. Sanz-Nogués, D. I. Zeugolis, P. Dockery, T. O'Brien, A. Pandit, *Biomaterials* **2014**, *35*, 8757.
[289] S. Babu, F. Albertino, A. Omidinia Anarkoli, L. De Laporte, *Adv. Healthcare Mater.* **2021**, *10*, 2002221.
[290] A. Mandal, J. R. Clegg, A. C. Anselmo, S. Mitragotri, *Bioeng. Transl. Med.* **2020**, *5*, e10158.
[291] A. S. Hoffman, *Adv. Drug Delivery Rev.* **2013**, *65*, 10.

[292] A. Vashist, A. Kaushik, A. Vashist, J. Bala, R. Nikkhah-moshaie, M. Nair, N. Delhi, **2019**, *23*, 1436.
[293] S. V. Vinogradov, E. V. Batrakova, A. V. Kabanov, *Bioconjugate Chem.* **2004**, *15*, 50.
[294] Y. Ma, Y. Ge, L. Li, *Mater. Sci. Eng., C* **2017**, *71*, 1281.
[295] I. W. Y. Mak, N. Evaniew, M. Ghert, *Am. J. Transl. Res.* **2014**, *6*, 114.
[296] Q. Q. Yin, L. Wu, M. L. Gou, Z. Y. Qian, W. S. Zhang, J. Liu, *Acta Anaesthesiol. Scand.* **2009**, *53*, 1207.
[297] J. Li, D. J. Mooney, *Nat. Rev. Mater.* **2016**, *1*, 16071.
[298] J. Guan, N. Ferrell, L. J. Lee, D. J. Hansford, *Biomaterials* **2006**, *27*, 4034.
[299] Y. Hu, Q. Wang, J. Wang, J. Zhu, H. Wang, Y. Yang, *Biomicrofluidics* **2012**, *6*, 026502.
[300] Y. Nishizawa, S. Matsui, K. Urayama, T. Kureha, M. Shibayama, T. Uchihashi, D. Suzuki, *Angew. Chem., Int. Ed.* **2019**, *58*, 8809.
[301] A. Mourran, Y. Wu, R. A. Gumerov, A. A. Rudov, I. I. Potemkin, A. Pich, M. Möller, *Langmuir* **2016**, *32*, 723.
[302] K. Akiyoshi, S. Kobayashi, S. Shichibe, D. Mix, M. Baudys, S. Wan Kim, J. Sunamoto, *J. Controlled Release* **1998**, *54*, 313.
[303] S. V. Vinogradov, T. K. Bronich, A. V. Kabanov, *Adv. Drug Delivery Rev.* **2002**, *54*, 135.
[304] J. P. Rolland, B. W. Maynor, L. E. Euliss, A. E. Exner, G. M. Denison, J. M. DeSimone, *J. Am. Chem. Soc.* **2005**, *127*, 10096.
[305] S. Xu, Z. Nie, M. Seo, P. Lewis, E. Kumacheva, H. A. Stone, P. Garstecki, D. B. Weibel, I. Gitlin, G. M. Whitesides, *Angew. Chem., Int. Ed.* **2005**, *44*, 724.
[306] D. Dendukuri, K. Tsoi, T. A. Hatton, P. S. Doyle, *Langmuir* **2005**, *21*, 2113.
[307] U. Hasegawa, S. I. M. Nomura, S. C. Kaul, T. Hirano, K. Akiyoshi, *Biochem. Biophys. Res. Commun.* **2005**, *331*, 917.
[308] A. Omidinia-Anarkoli, S. Boesveld, U. Tuvshindorj, J. C. Rose, T. Haraszti, L. De Laporte, *Small* **2017**, *13*, 1702207.

Yonca Kittel (née Kayku) obtained her Master's degree in chemistry from RWTH Aachen University, Germany. She is currently working on her doctoral studies at DWI-Leibniz Institute for Interactive Materials under the guidance of Prof. Laura De Laporte and Prof. Alexander J. C. Kuehne. Her work focuses on the microfluidic synthesis of multifunctional microgels for treatment of inflammatory bowel syndrome.

Alexander J.C. Kuehne is a full professor for macromolecular and organic chemistry at Ulm University and an associated scientist at DWI—Leibniz Institute for Interactive Materials. His research interests evolve around molecular and colloidal materials for photonic and biomedical applications.

Laura De Laporte designs advanced biomedical systems that control and direct the interaction with cells. She is a chemical engineer from Ghent and did her Ph.D. at Northwestern University. After a post doc at EPFL in life science, she joined the DWI-Leibniz Institute for Interactive Materials. In 2018, she became a Leibniz professor at the RWTH University in Aachen, Germany, bridging the Chemistry Department and University Hospital. Her team designs low-invasive, polymeric regenerative hydrogels that orient after injection to repair and grow anisotropic tissues. In addition, dynamic hydrogels are created to study mechanobiology.